On the Signalling Length in Digital Wireless Communications

by

Guangran Zhu

B.Sc.E., University of New Brunswick, 2003

A Thesis Submitted in Partial Fulfillment of the Requirements for the Degree of

Master of Science in Engineering

in the Graduate Academic Unit of Electrical Engineering

Supervisors:	Brent R. Petersen, B.Eng., M.A.Sc., Ph.D. Bruce G. Colpitts, B.Sc.E., M.Sc.E., Ph.D.
Examining Board:	R. Tervo, B.Sc., M.Sc., Ph.D., Chair K. B. Englehart, B.Sc.E., M.Sc.E., Ph.D. O. Kaser, B.C.S.S., M.S., Ph.D., External examiner J. Meng, B.Sc.E., M.Sc., Ph.D.

This thesis is accepted by the
Dean of Graduate Studies

THE UNIVERSITY OF NEW BRUNSWICK

August, 2005

To my parents, Wenzhao Zhu and Huixian Yan.

To the memory of my grandparents.

Abstract

Traditionally, multiple antennas are separated on the scale of carrier wavelength to achieve diversity gain, antenna gain, and spatial multiplexing. A similar parameter, signalling length is proposed to constrain antenna separation in line-of-sight pure delay channels to achieve spatial multiplexing. The performance improvement is demonstrated through the use of condition numbers of the complex baseband channel matrix.

Acknowledgement

I would like to express my sincere gratitude to my supervisors, Dr. Brent R. Petersen for his guidance and encouragement which made this work a possibility, and to Dr. Bruce G. Colpitts who pulled me out on numerous occasions when my research appeared stagnant. Both of them have been patient to accommodate the natural development of my research style, and provide consistent support for planning my career development. For which, I am very grateful.

This research was supported by the Atlantic Innovation Fund from the Atlantic Canada Opportunities Agency, and by Aliant, our industrial partner.

I would also like to thank the technical staff in the department, particularly Blair Allen, Kevin Hanscom, and Bruce Miller, who generously shared knowledge to help me construct the channel measurement system, and the office staff Karen Annett, Denise Burke, and Shelley Cormier for their kindness and warmth which made my stay and work a pleasant experience.

Finally, I sincerely thank my parents for their enduring love, support, and encouragement throughout my studies thousands of miles away from home.

Table of Contents

VITA

List of Tables

List of Figures

List of Abbreviations

BER	Bit Error Rate
BS	Base Station
CCI	Co-channel Interference
CDMA	Code Division Multiple Access
ISI	Intersymbol Interference
LMCS	Local Multipoint Communication Systems
LOS	Line of Sight
MRC	Maximum Ratio Combining
OC	Optimum Combining
SC	Selection Combining
SINR	Signal-to-Interference-plus-Noise Ratio
SNR	Signal-to-Noise-Ratio
TDMA	Time Division Multiple Access
UWB	Ultra Wideband
ZF	Zero-Forcing

List of Symbols

$\|\bullet\|$	Matrix norm operator
$\bullet^{-1}$	Complex inverse operator
$\bullet^{H}$	Hermitian operator
$\otimes$	Convolution operator
$E[\bullet]$	Expectation operator
c	Speed of light
$c_{ji}(t)$	Signal after the j^{th} receive filter in the i^{th} equalizer
$d_i[n]$	Transmitted data from the i^{th} portable
$\hat{d}_i[n]$	Sampled data before the quantizer
$\widetilde{d}_i[n]$	Estimate of transmitted data
f_c	Carrier frequency
f_g	Signalling rate
f	Dummy parameter used as a frequency index
$g(t)$	Impulse response of the transmit filter
$g(-t)$	Impulse response of the ideal non-causal matched filter
$G(f)$	Frequency response of the transmit filter
$h_{ij}(t)$	Impulse response of the wireless channel from the i^{th} portable to the j^{th} receive antenna
$H(f)$	Complex baseband channel matrix
$H_{ij}(f)$	Frequency response of the wireless channel from the i^{th} portable

	to the j^{th} receive antenna
i	Dummy parameter used as a portable or a linear equalizer index
j	Dummy parameter used as a receive antenna index
k	Dummy parameter used as a discrete time shifting index
l_{ij}	Distance between the i^{th} portable and the j^{th} receive antenna
L	Number of bits mapped to a symbol in linear modulation scheme
M	Number of base station antennas
n	Dummy parameter used as a discrete time index
N	Number of portable antennas
q	Dummy parameter used as a portable index
$s_j(t)$	Received signal at the j^{th} receive antenna
t	Dummy parameter used as a continuous time index
$r_i(t)$	Impulse response of the i^{th} equalizer
$r_{ji}(t)$	Impulse response of the j^{th} equalizer filter in the i^{th} equalizer
$R(f)$	Equalizer matrix
$R_i(f)$	Frequency response of the i^{th} equalizer
$R_{ji}(f)$	Frequency response of the j^{th} equalizer filter in the i^{th} equalizer
T_I	Delay difference at the first receive antenna
T_{II}	Delay difference at the second receive antenna
T_g	Signalling period
$u_i(t)$	Transmitted signal of the i^{th} portable
$v_i(t)$	Combined signal after the receive filters in the i^{th} equalizer

$w_i(t)$	Signal after the i^{th} equalizer before the sampler
x	Dummy integer
X	Gaussian random variable
$X(t)$	Gaussian random process
Y	Gaussian random variable
$Y(t)$	Gaussian random process
Z_j	Interference at the sampler of the j^{th} branch
$\beta_i(f)$	Phase difference at the j^{th} receive antenna
$\delta[i]$	Kronecker delta function
Δ	Antenna separation
θ_i	Angle of the i^{th} portable
λ_c	Carrier wavelength
λ_g	Signalling length
μ_d	Mean of the transmitted data
ρ	Correlation coefficient
σ_d^2	Variance of the transmitted data
τ_{ij}	Path delay between the i^{th} portable and the j^{th} receive antenna
$\phi_{dd}(k)$	Autocorrelation function of the transmitted data
$\Phi_{dd}(f)$	Power spectral density function of the transmitted data
$\phi_{uu}(t,\tau)$	Autocorrelation function of the transmitted signal
$\bar{\phi}_{uu}(\tau)$	Time averaged autocorrelation function of the transmitted signal

$\overline{\Phi}_{uu}(f)$	Time averaged power spectral density function of the transmitted signal

Chapter 1 Introduction

1.1 Background and Literature Review

There is an increasing service demand on digital radio communications. Harsh wireless channels always present many difficulties to engineers when designing these systems. One major impediment is the small scale fading due to the multipath effects[1]. Unlike wired channels that provide isolated point to point connections, the wireless channels usually involve many reflecting objects around the transmit antennas, around the receive antennas, and between them. A signal is bounced through several paths before reaching the receive antennas. This results in several copies of the signal which undergo different attenuations and phase shifts, i.e. time delays, at the time of reception. These copies are superimposed either constructively or destructively, and cause rapid fluctuations of the received signal strength over very short travel distances.

The carrier wavelength serve as the parameter to quantify the distance over which the received signals may vary significantly. The reasoning behind the use of this parameter assumes that the signal bandwidth is narrow with respect to the carrier frequency, f_c. When being transmitted, the signal can be well approximated as a pure sinusoid, e.g. $\cos(2\pi f_c t)$. Due to the multipath effects, the received signal becomes

$$X(t)\cos(2\pi f_c t) - Y(t)\sin(2\pi f_c t), \tag{1.1.1}$$

1. Small scale fading is due to the multipath effects, motion of the portables, and motion of surrounding objects. Multipath effects only cause different signal strengths at different locations, but the environment should be considered deterministic. However, many publications refer to small scale fading as the multipath effects while not explicitly stating the effect of motion.

where $X(t)$ and $Y(t)$ are narrowband Gaussian random processes. At every time instance, X and Y are zero mean, equal variance, independent Gaussian random variables. The envelope of the signal $\sqrt{X^2 + Y^2}$ is a random variable with Rayleigh distribution [Jak94, ch. 1].

Clake showed that the correlation of the signal envelopes from two antennas is almost zero if they are separated by half of a carrier wavelength in an environment with many reflecting objects [Cla68]. An intuitive understanding of the reasoning behind the use of carrier wavelength is from the standing wave pattern in a transmission line. When the line is either open or short terminated, the standing wave has sharp nulls every half wavelength. That is analogous to the significant variation in signal strength when a receive antenna moves over this distance.

One way to combat small scale fading is to have multiple receive antennas. The premise is that if they are all separated on the scale of carrier wavelength, it is unlikely to have low signal strength at all antennas simultaneously. Since the signal envelopes are uncorrelated random variables, we can select the antenna with the strongest signal strength for later detection. This technique is known as the selection combining (SC) method. The improvement, known as the diversity gain, is a reduction of the variance of the signal-to-noise ratio (SNR) after selection. In the limiting case, the probability density function of the SNR becomes a delta function with zero variance, and centers at the local mean of the SNR.

Another way to combat small scale fading is to apply a weight which is equal to the signal-voltage-to-noise-power ratio of each receiving antenna, and coherently combine the signals. This technique is known as the maximum ratio combining

(MRC) method. The SNR after combining is the sum of the SNRs of the receive antennas. The improvement, known as the antenna gain, is a shift of the probability density function of the SNR. In the limiting case, all the radiated power is collected at the receive antennas. In theory, there is no limitation on antenna separation to achieve antenna gain as long as noise at each branch is uncorrelated with others. It is possible to achieve both diversity gain and antenna gain if we separate receive antennas on the scale of carrier wavelength and perform MRC.

We have presented the techniques to achieve diversity gain and antenna gain in order to combat small scale fading in micro-scale systems. They are also applicable in macro-scale systems in which antennas are widely separated. An example where macro-scale systems achieve diversity gain is the current cellular system. If a portable phone detects signals from multiple base stations (BS), it selects the one with the highest strength. An example where macro-scale systems achieve antenna gain is the distributed antenna system. The signal from a portable phone is detected by a few receive antennas simultaneously. The signals are centrally combined through MRC[2]. It is apparent that the separation on the scale of carrier wavelength is satisfied by default in macro-scale systems.

The discussion above has implicitly assumed a noise-limited environment. As more and more portables demand wireless services, they more likely transmit over the same frequency band at the same time and create co-channel interference (CCI). For time division multiple access (TDMA) systems, CCI could be the signals from portables in other cells. For code division multiple access (CDMA) systems, CCI is

2. A delay element is assumed at each antenna to bring the signals to synchronism at the moment of combining.

an inherent problem since the frequency reuse factor is one in every cell. CCI has become the dominant factor that degrades the system performance rather than noise in new wireless systems.

Multiple antennas can also be used to combat interference in an interference-limited environment. If the BS has one antenna, we cannot spatially separate the signal from its CCI. TDMA systems rely on the assumption that the interference is close to the noise floor, and CDMA systems rely on the spreading code. However, if the BS has two receive antennas, the superposition of signals from the portables at one receive antenna is likely different from the superposition at the other receive antenna. We can exploit this difference to identify the desired signal from other interfering signals. This is achieved through optimum combining (OC) in the presence of flat fading [Win84, Win87] or optimum equalization in the presence of frequency selective fading [Cla94]. In general *M* receive antennas can suppress *M-1* interferers, and the performance improvement is known as spatial multiplexing [Pau03, ch 2][3]. We notice it is possible to achieve diversity gain and antenna gain simultaneously, but it is impossible to achieve spatial multiplexing with the other two simultaneously [Zhe03].

Winters in [Win87] states: “The receiver can suppress interfering signals and enhance desired signal reception as long as the received desired signal powers and phases differ somewhat from the received interfering signal powers and phases at

3. It should be noted that spatial multiplexing is different from interference reduction in [Pau03, ch 2]. Spatial multiplexing requires perfect channel knowledge at the receiver or the transmitter usually gained through training, and is not dependent on the radiation pattern of the antenna array. Interference reduction refers to steering the main lobe of the radiation pattern to the desired user and nulls to interferers, i.e. beamforming.

more than one antenna." In essence, the difference in the signal strength and phase are the two properties an optimum filter can exploit. Consider the signal strength only. The research after Clarke's theoretic analysis has confirmed uncorrelated fading between antennas separated on the scale of carrier wavelength in various channel conditions and frequency bands (see [Ert98] and the reference therein). Also, Vaughan and Scott [Vau93] showed that envelope correlations for closely spaced monopoles were much lower than predicted in [Cla68] due to the mutual coupling between antennas. Therefore, in most cases, optimum filter could achieve spatial multiplexing by exploiting the signal strength without worrying about the difference in phase.

This thesis investigates the effect of phase on achieving spatial multiplexing. With line-of-sight (LOS) pure delay channels, if we insist on separating antennas on the scale of carrier wavelength, the superposition of signals will be almost identical. Having multiple antennas is the same as having one, and it is impossible to separate signals. If the separation is very large, the superposition of signals will be different due to difference in delays along the paths. The motivation behind this thesis work is to quantify the antenna separation using LOS pure delay channels. Once this problem is understood, more complex channel conditions can be applied, and the separation between antennas can be appropriately designed.

An important publication is by Yanikomeroglu et al. [Yan02][4]. The authors analyzed the effect of interference correlation on antenna gain in a distributed antenna CDMA system. Since noise is uncorrelated, MRC yields an SNR being the sum of

4. When we mention the work by Yanikomeroglu et al. throughout this thesis, we refer to [Yan02].

the SNR of all antenna branches. In the presence of multiple portables, the interference is correlated given that the antenna separation is on the order of carrier wavelength. Therefore, the signal-to-interference-plus-noise ratio (SINR) out of the combiner is no longer the sum of the branch SINR. The authors first calculated the correlation coefficient of the interference in a two-portable two-receive antenna scenario. Next, they identified the region in which the presence of a second portable would incur high envelope correlation and named it the *caution zone*. Then, they proposed the term *chiplength* ([speed of light]/[chip rate]) of the spreading code. They showed the ratio between the length of the square service region to chiplength affects the density of the caution zone. And for a given ratio, the density of the caution zone is again affected by the separation of antennas. This establishes the relation between antenna separation and the chiplength.

Table 1.1.1 summarizes the measuring scales of antenna separation that are sufficient to achieve different gains through use of multiple antennas in noise-limited and interference-limited environments with many reflecting objects.

1.2 Thesis Contribution

A different term *signalling length* ([speed of light]/[signalling rate]) is proposed in this thesis. And it is apparent that our signalling length corresponds to the chiplength for CDMA systems. The major contribution of this work and the work by Yanikomeroglu et al. is the idea of comparing the antenna separation to the signalling length, and constraining separation between antennas to at least greater than one signalling length in order to combat interference. However, there are two major differences between our work and their work:

	Noise-limited		Interference-limited		
	Diversity gain (SC)	Antenna gain (MRC)	Diversity gain (SC)	Antenna gain (MRC)	Spatial Multiplexing (OC)
Micro-scale system	Carrier wavelength	Carrier wavelength	Carrier wavelength	No gain	Carrier wavelength
Macro-scale system	Carrier wavelength	Carrier wavelength	Carrier wavelength	Chip-length	Carrier wavelength

Table 1.1.1 Measuring scales of antenna separation to achieve different gains.

1. We start with exploring spatial multiplexing from multiple antennas, while Yanikomeroglu et al. start with exploring antenna gain. Therefore, the receiver in our work is an optimum equalizer followed by a matched filter, instead of a correlator followed by a combiner to perform MRC.
2. The different structures of the receivers determine the use of different parameters to reflect the effect of large antenna separation. We adopt the mean of the condition number of the channel matrix instead of the correlation coefficient of the interference.

1.3 Thesis Structure

There are four chapters in this thesis. Chapter 2 establishes the system model. Multiple portables each equipped with one antenna are in communication simultaneously with multiple antennas connected to one BS. The equalizer and the matched filter are separated in the model in order to match up the channel-equalizer pair. The zero-forcing (ZF) optimization criterion is adopted for the equalizer, and it is shown that a ZF equalizer inverts the channel matrix to suppress all interference. This paves the way to further justify the use of condition numbers of the channel matrix in the next chapter.

Chapter 3 covers the reasoning to constrain antenna separation to be greater than one signalling length. Since an equalizer inverts the channel matrix, a better channel matrix due to large antenna separation suggests an easier to achieve operating point for the equalizer. The mean of the condition number is used to show the good and bad channel matrix at different antenna separations. An analysis using correlated interference, similar to the work of Yanikomeroglu et al., but modified to our

non-spread system model is also presented. The potential applications of the concept of signalling length in digital wireless communications is subsequently discussed.

Chapter 4 summarizes the thesis and points out potential research directions.

Chapter 2 System Model and Zero-forcing Linear Equalizer

This chapter presents the reverse link scenario in a multiple portable digital communication system and the corresponding system model. The linear equalizers used inside the BS receivers are optimized according to the ZF criterion. We will show that computing these equalizers is equivalent to inverting the baseband channel matrix over the Nyquist bandwidth.

2.1 System Model

We consider the scenario in which there are multiple portables transmitting simultaneously to one central BS. Each portable is equipped with one antenna, and the BS is equipped with multiple antennas. All antennas are considered omni directional. This model also assumes a linear modulation scheme. Thus, for mathematical convenience, we will only deal with the transmission of the equivalent baseband signals through baseband channels [Pro95, ch. 4].

A block diagram of the major components of the system is shown in Fig.2.1.1; i, j, are the indices for the N portables and the M BS antennas respectively; $d_i[n]$ is the transmitted data from the i^{th} portable; $g(t)$ is the impulse response of the transmit filter; $u_i(t)$ is the transmitted signal; $h_{ij}(t)$ is the impulse response of the wireless channel from the i^{th} portable to the j^{th} receive antenna; $s_j(t)$ is the received signal; $\widetilde{d}_i[n]$ is the output of the i^{th} BS receiver, an estimate of the transmitted data $d_i[n]$.

2.1.1 Portables

The portables transmit information encoded in digital form. In general, a digital

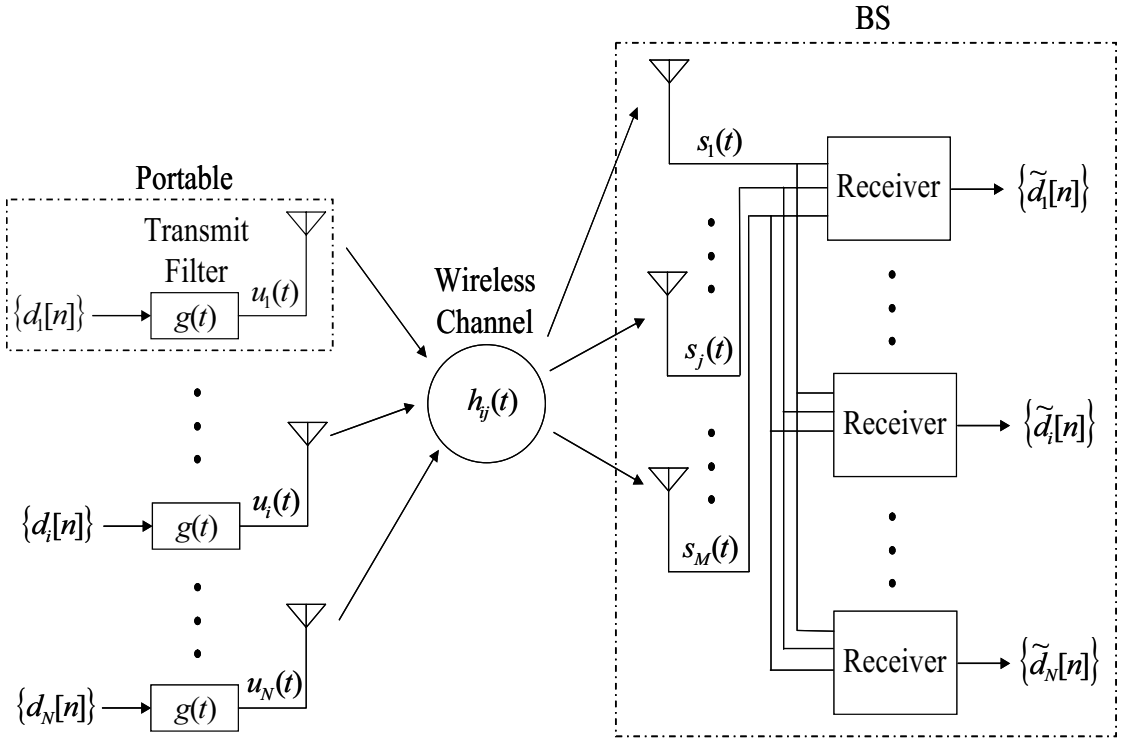

Figure 2.1.1 Block diagram of the reverse link
of a multiple portable system.

modulator can map L binary bits to a symbol and perform modulation, such as quadrature amplitude modulation, to increase spectral efficiency. This requires notation in the complex domain. We use the simplest binary modulation to keep all the notation in the real domain. Without loss of generality, our result is applicable to any digital system using complex modulation.

The transmitted data, $d_i[n]$, are modeled as independent identically distributed equi-probable Bernoulli random variables. They are real, have zero mean, unit variance, and are mutually uncorrelated in time. These are expressed as

$$d_i[n] \in \{-1,+1\}, \tag{2.1.1}$$

$$\mu_d = E[d_i[n]] = 0, \tag{2.1.2}$$

$$\sigma_d^2 = E[d_i^2[n]] = 1, \tag{2.1.3}$$

$$\phi_{dd}(k) = E[d_i[n]\, d_i[n+k]] = \sigma_d^2 \delta[k], \tag{2.1.4}$$

where k is an integer to denote a shift in time, and $\delta[k]$ is the Kronecker delta function defined as

$$\delta[k] = 1, \text{ where } k = 0, \tag{2.1.5a}$$

$$\text{and } \delta[k] = 0, \text{ otherwise.} \tag{2.1.5b}$$

They are also mutually uncorrelated across portables

$$E[d_i[n]\, d_q[n]] = \sigma_d^2 \delta[i-q], \tag{2.1.6}$$

where q is another index for the N portables. The power spectral density of (2.1.4) is

$$\Phi_{dd}(f) = \sigma_d^2. \tag{2.1.7}$$

The signalling period T_g is the time lag between two consecutive symbols, and (2.1.7) can be regarded as being periodic in f with a period $1/T_g$. Throughout this thesis, a

Fourier transform pair will have time-domain and frequency-domain functions denoted by the lower-case and the corresponding upper-case letters respectively.

The signalling length λ_g and the signalling frequency f_g are defined respectively as

$$\lambda_g = cT_g\,, \tag{2.1.8}$$

$$f_g = \frac{c}{\lambda_g}\,, \tag{2.1.9}$$

where c is the speed of light. The term signalling length is newly defined here, and it will be shown that it is the key parameter against which the antenna separation should be specified.

The transmit filter $g(t)$ is assumed to be the ideal bandlimiting Nyquist filter defined as [Skl01, ch. 3]

$$g(t) = \frac{\sin(\frac{\pi t}{T_g})}{\frac{\pi t}{T_g}}\,, \tag{2.1.10}$$

and its frequency-domain expression is

$$G(f) = \mathrm{rect}\left(\frac{f}{f_g}\right) = T_g\,, \text{ where } f \in \left[-\frac{1}{2T_g}, +\frac{1}{2T_g}\right], \tag{2.1.11a}$$

$$\text{and} \quad G(f) = 0, \text{ otherwise.} \tag{2.1.11b}$$

The transmitted signal $u_i(t)$ can be expressed as

$$u_i(t) = \sum_{n=-\infty}^{+\infty} d_i[n]\, g(t - nT_g). \tag{2.1.12}$$

Its mean value is

$$\mu_u(t) = \sum_{n=-\infty}^{+\infty} E[d_i[n]]\, g(t - nT_g), \tag{2.1.13}$$

which is zero due to (2.1.2). Its autocorrelation function is

$$\begin{aligned} \phi_{uu}(t,\tau) &= E[u(t)u(t+\tau)] \\ &= \sum_{n=-\infty}^{+\infty}\sum_{k=-\infty}^{+\infty} E[d_i[n]d_i[n+k]]\, g(t - nT_g)\, g(t+\tau-(n+k)T_g) \\ &= \sum_{k=-\infty}^{+\infty} \phi_{dd}(k) \sum_{n=-\infty}^{+\infty} g(t - nT_g)\, g(t+\tau-(n+k)T_g). \end{aligned} \tag{2.1.14}$$

The $\mu_u(t)$ expression given in (2.1.13) shows that $u_i(t)$ is periodic in mean with period T_g, and the $\phi_{uu}(t,\tau)$ expression in (2.1.14) shows that the autocorrelation function of $u_i(t)$ is periodic in both time t, and delay τ with period T_g. Thus, the transmitted signal $u_i(t)$ is a cyclostationary process. The power spectral density of $u_i(t)$ would have been a function of two variables. In order to carry out the analysis in the frequency domain, the autocorrelation function is averaged in time

$$\overline{\phi}_{uu}(\tau) = \frac{1}{T_g} \int_{-\frac{T_g}{2}}^{+\frac{T_g}{2}} \phi_{uu}(t,\tau)\, dt\ . \tag{2.1.15}$$

The Fourier transform of (2.1.15) gives the time averaged power spectral density of $u_i(t)$ [Pro95, ch. 4]

$$\overline{\Phi}_{uu}(f) = \frac{\sigma_d^2}{T_g}\left|G(f)\right|^2, \text{ where } f \in \left[-\frac{1}{2T_g}, +\frac{1}{2T_g}\right], \tag{2.1.16a}$$

$$\text{and } \overline{\Phi}_{uu}(f) = 0, \text{ otherwise.} \tag{2.1.16b}$$

The signals from all portables share the same power spectral density function. There will be a desired signal to be extracted at the BS, while other signals are

considered as CCI.

2.1.2 Wireless Channels

The wireless channel is assumed to be quasi-static during transmission. Since the portables are transmitting simultaneously, the system is limited by interference and the effect of noise is omitted [Yan02]. The frequency-domain $N \times M$ channel matrix becomes

$$H(f) = \begin{bmatrix} H_{11}(f) & \dots & H_{1M}(f) \\ \vdots & H_{ij}(f) & \vdots \\ H_{N1}(f) & \dots & H_{NM}(f) \end{bmatrix}, \tag{2.1.17}$$

where $H_{ij}(f)$ corresponds to the channel from the i^{th} portable to the j^{th} receive antenna.

2.1.3 Base Station Receivers

The received signal at each antenna is a superposition of signals from all portables. It is expressed as

$$s_j(t) = \sum_{i}^{N} u_i(t) \otimes h_{ij}(t), \tag{2.1.18}$$

where $\otimes$ denotes the convolution operator. The BS relies on N parallel receivers to simultaneously process the received signals and produce estimates of the transmitted data.

2.2 Zero-forcing Linear Equalizers

Each one of the N parallel BS receivers contains a linear equalizer. This section establishes that optimizing the linear equalizers according to the ZF criterion is equivalent to inverting the baseband channel matrix.

2.2.1 Linear Equalizers

The linear equalizer uses spatially separated antennas to suppress CCI and uses

temporal filters to process the signals at the antenna branches before the signals are combined. Thus, it is sometimes referred as a space-time processor or a space-time linear equalizer [Fal00]. It in essence compensates for the distortion introduced by the channel, and restores the property of the desired signal through equalization.

Fig. 2.2.1 shows the details of BS receivers; $r_{ji}(t)$ is the impulse response of the j^{th} filter in the i^{th} equalizer; the i^{th} equalizer $r_i(t)$ is a $M \times 1$ column vector

$$\begin{bmatrix} r_{1i}(t) \\ \vdots \\ r_{ji}(t) \\ \vdots \\ r_{Mi}(t) \end{bmatrix};$$

$v_i(t)$ is the combined output after the equalizer; the ideal non-causal filter $g(-t)$ is matched to the transmit filter $g(t)$; the output $w_i(t)$ is sampled at nT_g, and the soft estimate $\hat{d}_i[n]$ is quantized to yield the hard decision $\tilde{d}_i[n]$.

The transmit filter $g(t)$ and the matched filter $g(-t)$ bandlimit the spectral contents of all signals to the Nyquist bandwidth, $[-1/2T_g, +1/2T_g]$. The question is to find the right equalizer filters $r_{ji}(t)$, thus the equalizers, so that the estimated $\tilde{d}_i[n]$ is the same as the actual transmitted $d_i[n]$.

2.2.2 Zero-forcing Optimization Criterion

There exist a few optimization criteria according to which the equalizers can be found, and the digital system operating with those equalizers will be optimal in the sense of that criterion. The ZF criterion is one of them [Shn67]. It dictates that all interference is completely suppressed, and the exact transmitted signal is detected at the sampler. The equalizers optimized according to it generally do not yield the best

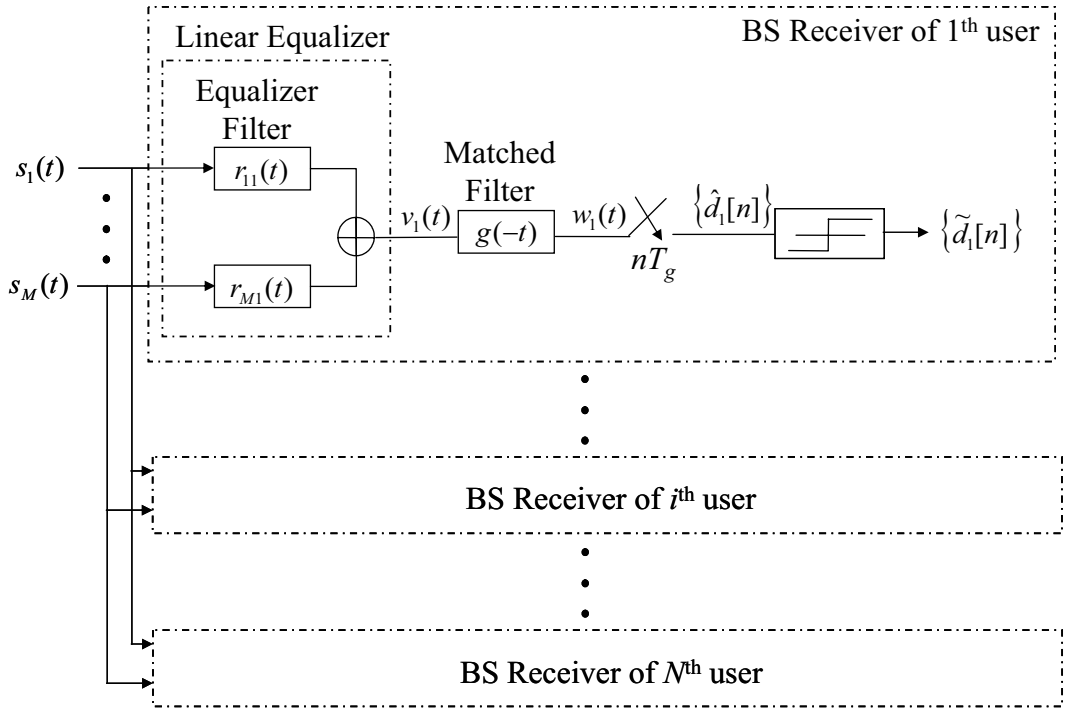

Figure 2.2.1 BS receiver and the linear equalizer.

system performance [Sal93]. This is because an equalizer optimized for a specific symbol is not likely to be good for estimating subsequent symbols in the presence of random noise. At the time to detect the second symbol, the equalizer may cause significant noise enhancement which renders accurate detection. However, the ZF criterion serves the purpose of showing the existence of an effective system operating point, and they can be further optimized by other statistical criteria, such as the minimimum mean squared error criterion. We use the ZF criterion because it gives an intuitive interpretation of equalization in the frequency domain. This interpretation suggests to evaluate the channel matrix using condition numbers in the following chapter.

Consider the system model shown in Fig. 2.2.2 in which there is only one receive antenna. We want to detect the signal from the first portable, and signals from all other portables are regarded as CCI. The equalized combined channel of the first portable to the sampler including the transmit filter, the channel, the equalizer filter, and the matched filter, is

$$p_{11}(t) = g(t) \otimes h_{11}(t) \otimes r_{11}(t) \otimes g(-t), \tag{2.2.1}$$

and the equalized combined co-channels of all other portables are

$$p_{i1}(t) = g(t) \otimes h_{i1}(t) \otimes r_{11}(t) \otimes g(-t), \text{ where } \; i \in [2, N]. \tag{2.2.2}$$

Expressed in the frequency domain, (2.2.1) and (2.2.2) become

$$P_{i1}(f) = G(f) H_{i1}(f) R_{11}(f) G^*(f),$$

$$\text{where } \; i \in [1, N] \; \text{ and } f \in (-\infty, +\infty). \tag{2.2.3}$$

There are two kinds of interference the ZF linear equalizers need to suppress. The

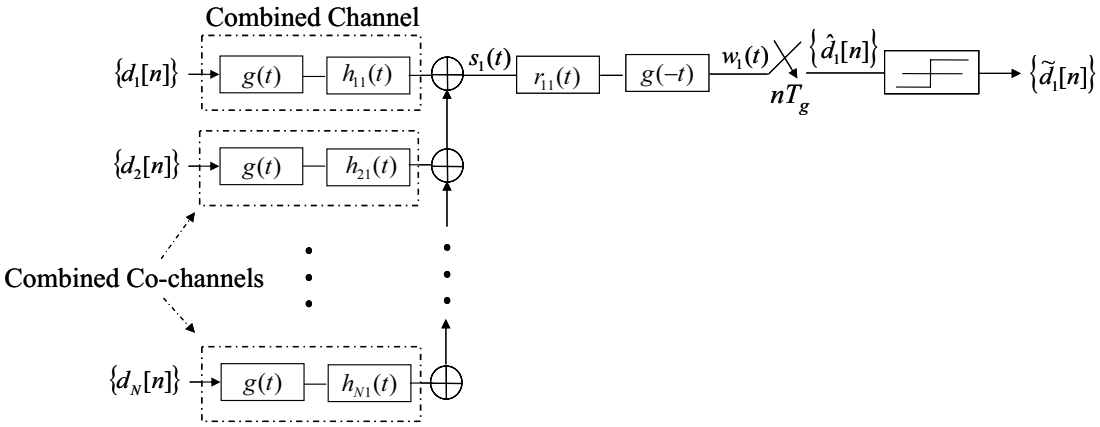

Figure 2.2.2 System model with one receive antenna.

intersymbol interference (ISI) is due to the smearing effect of the channel. Some energy of the transmitted data symbol leaks to the following symbols. The time-domain condition for zero ISI is [Shn67]

$$p_{11}(nT) = \delta[n]. \tag{2.2.4}$$

The time-domain condition for zero CCI which is due to the sharing of the bandwidth with other portables is

$$p_{i1}(nT) = 0\text{, where } i \in [2, N]. \tag{2.2.5}$$

These time-domain conditions (2.2.4) and (2.2.5) can be expressed together in the frequency domain as

$$\frac{1}{T_g}\sum_{b=-\infty}^{+\infty} P_{i1}\left(f + \frac{b}{T_g}\right) = \delta[i-1]\text{, where } i \in [1, N] \text{ and } f \in (-\infty, +\infty). \tag{2.2.6}$$

Substituting $P_{i1}(f)$ from (2.2.3) into (2.2.6) gives

$$\frac{1}{T_g}\sum_{b=-\infty}^{+\infty} G\left(f + \frac{b}{T_g}\right) H_{i1}\left(f + \frac{b}{T_g}\right) R_{11}\left(f + \frac{b}{T_g}\right) G^*\left(f + \frac{b}{T_g}\right) = \delta[i-1],$$

$$\text{where } i \in [1, N] \text{ and } f \in (-\infty, +\infty). \tag{2.2.7}$$

From the conditions of the bandlimiting Nyquist filter $g(t)$ in (2.1.11a) and (2.1.11b), (2.2.7) becomes

$$H_{i1}(f) R_{11}(f) = \frac{1}{T_g}\delta[i-1],$$

$$\text{where } i \in [1, N] \text{ and } f \in \left[-\frac{1}{2T_g}, +\frac{1}{2T_g}\right]. \tag{2.2.8}$$

If there is only one portable with no CCI, (2.2.8) is one equation with one unknown $R_{11}(f)$ and there is likely a solution. If two portables are transmitting, one desired

and one CCI, (2.2.8) becomes two equations with one unknown. There will not likely be a solution. It is impossible to suppress the CCI. However, adding another receive antenna introduces freedom, $R_{21}(f)$. The sum of the two paths going through the two receive antennas may satisfy both the zero ISI condition

$$H_{11}(f)R_{11}(f)+H_{12}(f)R_{21}(f)=\frac{1}{T_g}\text{, where } f\in\left[-\frac{1}{2T_g},+\frac{1}{2T_g}\right], \quad (2.2.9)$$

and the zero CCI condition

$$H_{21}(f)R_{11}(f)+H_{22}(f)R_{21}(f)=0\text{, where } f\in\left[-\frac{1}{2T_g},+\frac{1}{2T_g}\right]. \quad (2.2.10)$$

Thus, there are two equations with two unknowns, and (2.2.9) and (2.2.10) will likely have a solution. This small example demonstrates that adding more antennas provides the ZF linear equalizer new degrees of freedom to suppress CCI. In general, this can be expressed as

$$H(f)R_1(f)=\begin{bmatrix}1/T_g\\0\\:\\:\\0\end{bmatrix}\text{, where } f\in\left[-\frac{1}{2T_g},+\frac{1}{2T_g}\right]. \quad (2.2.11)$$

If the number of portables is less than or equal to the number of receive antennas, i.e. $N \le M$, there generally exists at least one solution to (2.2.11).

We have presented the existence of the ZF linear equalizer to detect the first portable. The BS may have N parallel ZF linear equalizers, one for each portable. Identical analysis can be applied to show the existence of the equalizers for other portables. Applying the similar expression of (2.2.11) for other ZF linear equalizers,

we get the matrix form representation of the ZF criterion as

$$H(f)R(f) = \begin{bmatrix} 1/T_g & \cdots & 0 \\ \vdots & & \vdots \\ \vdots & 1/T_g & \vdots \\ \vdots & & \vdots \\ 0 & \cdots & 1/T_g \end{bmatrix}, \tag{2.2.12}$$

where $R(f) = [R_1(f) \ \ldots \ R_N(f)]$, the $M \times N$ matrix of equalizers. In essence, the ZF linear equalizer effectively inverts the baseband channel matrix over $[-1/2T_g, +1/2T_g]$, and the bank of equalizers optimal in the ZF sense is

$$R(f) = \frac{1}{T_g} H(f)^{-1}, \tag{2.2.13}$$

where $\bullet^{-1}$ denotes the matrix inverse.

Chapter 3 Effect of Signalling Length

We have shown that the bank of ZF linear equalizers invert the baseband channel matrix over the Nyquist bandwidth. In this chapter, we will use line-of-sight (LOS) pure delay channels, and show the reasoning to constrain the separation of the receive antennas at the BS on the scale of signalling length. We will use condition numbers to demonstrate the improvement of the channel matrix. Next, we present the analysis of correlated interference similar to the work of Yanikomeroglu et al. but for a non-spread system. In the end, we will discuss the potential applications of signaling length in digital wireless communications.

3.1 Signalling Length in LOS channels

We concentrate on the case that two portables are in communication with two receive antennas, i.e. $N = M = 2$. The LOS pure delay scenario is shown in Fig. 3.1.1 (a). The two by two complex baseband channel matrix is

$$H(f) = \begin{bmatrix} e^{-j2\pi f\tau_{11}} & e^{-j2\pi f\tau_{12}} \\ e^{-j2\pi f\tau_{21}} & e^{-j2\pi f\tau_{22}} \end{bmatrix}, \text{ where } f \in \left[-\frac{1}{2T_g}, +\frac{1}{2T_g} \right], \tag{3.1.1}$$

and τ_{ij} denotes the path delay between the i^{th} portable and the j^{th} receive antenna. The path delays incur a linear phase difference at the first receive antenna, and it is

$$\beta_1(f) = 2\pi(\tau_{11} - \tau_{21})f \,. \tag{3.1.2}$$

Similarly, at the second receive antenna, it is

$$\beta_2(f) = 2\pi(\tau_{12} - \tau_{22})f \,. \tag{3.1.3}$$

The phase differences are linear functions with respect to frequency, and their

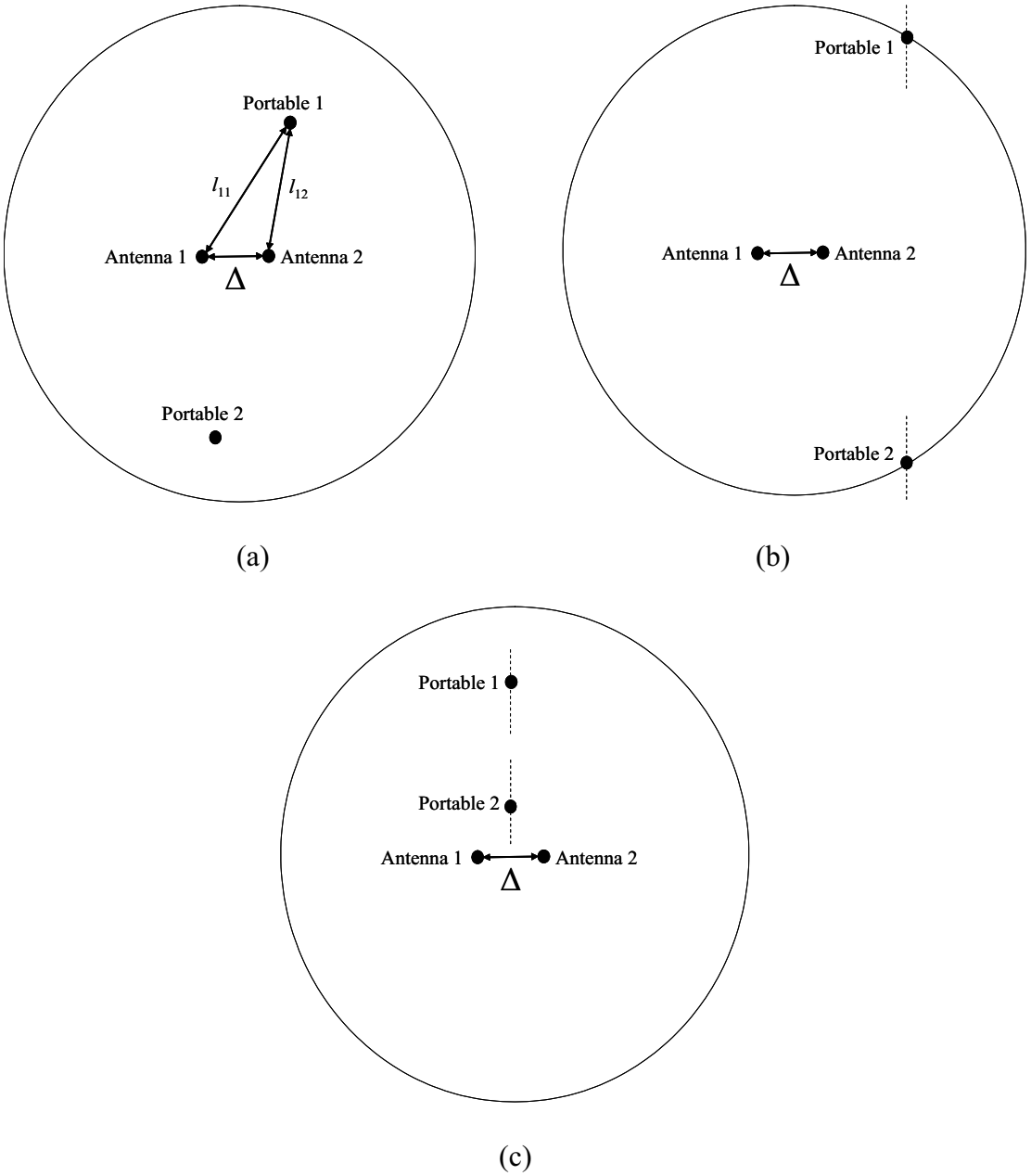

Figure 3.1.1 Two-portable two-receive-antenna scenarios,
(a) general case, (b) symmetry with respect to receive antennas,
(c) symmetry with respect to portables.

minimum and maximum values are determined by the minimum and maximum frequency. The ranges of the phase differences are limited by

$$\left|2\pi(\tau_{11}-\tau_{21})\frac{1}{2}f_g\right| > \beta_1(f), \tag{3.1.4}$$

and

$$\left|2\pi(\tau_{12}-\tau_{22})\frac{1}{2}f_g\right| > \beta_2(f). \tag{3.1.5}$$

If $\beta_1(f)$ and $\beta_2(f)$ are limited to a small range, the two received signals will be very similar. The maximum meaningful range for the phase differences is [-π, +π]. In order to fully exercise over this range, we have the relations

$$\left|2\pi(\tau_{11}-\tau_{21})\frac{1}{2}f_g\right| > \pi, \tag{3.1.6}$$

and

$$\left|2\pi(\tau_{12}-\tau_{22})\frac{1}{2}f_g\right| > \pi. \tag{3.1.7}$$

Let l_{ij} denote the actual distance between the i^{th} portable and the j^{th} receive antenna. Applying the relations $\tau_{ij} = l_{ij}/c$ and $f_g = c/\lambda_g$ to (3.1.6) and (3.1.7), we get

$$|l_{11}-l_{21}| > \lambda_g, \tag{3.1.8}$$

and

$$|l_{12}-l_{22}| > \lambda_g. \tag{3.1.9}$$

The expression in (3.1.8) states that the path lag between the two portables and the first receive antenna should be greater than one signalling length, and similiarly the expression in (3.1.9) states for the second receive antenna.

Without the knowledge of the portable locations, it is difficult to proceed.

However, if we switch the role of portables and receive antennas, we can rewrite (3.1.8) and (3.1.9) as

$$|l_{11} - l_{12}| > \lambda_g , \tag{3.1.10}$$

and

$$|l_{21} - l_{22}| > \lambda_g . \tag{3.1.11}$$

This is justified by the fact that the analysis is only concerned with the delay of the channels. There is no logical difference between portables and receive antennas in our model. The expression in (3.1.10) states that the path lag between the first portable to the two receive antennas should be greater than one signalling length, and similarly the expression in (3.1.11) states for the second portable.

The exact values of the path lags (l_{11}- l_{12}) and (l_{21}- l_{22}) are dependent on specific portable locations. Only when the angles of the portables relative to the BS receive antenna axis are around 0º do the path length differences approach the separation between receive antennas, Δ. In general, they are limited within

$$|l_{11} - l_{12}| < \Delta , \tag{3.1.12}$$

and

$$|l_{21} - l_{22}| < \Delta . \tag{3.1.13}$$

The receive antenna separation greater than the signalling length gives the freedom to some locations where the phase difference can fully exercise over [-π, +π]. This constraint is expressed as

$$\Delta > \lambda_g . \tag{3.1.14}$$

This is our basic result.

Hudson uses an expression similar to (3.1.14) to define wideband antenna arrays as those whose apertures are greater than the ratio [speed of light]/[signal bandwidth], which is the same as signalling length or chiplength [Hud81, ch. 2]. However, we are considering the separation between multiple omni directional antennas rather than antenna arrays for beamforming.

3.2 Additional Constraints

In addition to giving freedom to the phase differences, we also need to ensure that the slopes of the linear phase differences, $2\pi(\tau_{11}-\tau_{21})$ and $2\pi(\tau_{12}-\tau_{22})$ in (3.1.2) and (3.1.3), are not the same. If these slopes are identical, the phase differences of the two portables will be identical over the entire frequency range, and there is no difference we can exploit to achieve spatial multiplexing. Fig. 3.2.1 illustrates the phase differences with similar and different slopes. In addition, there are three pathological situations in which we get identical slopes: 1) when the portables are very close to each other, 2) when the portables are in symmetric locations with respect to the receive antennas as shown in Fig. 3.1.1 (b), and 3) when the receive antennas are in symmetric locations with respect to the portables as shown in Fig. 3.1.1 (c).

The constraint in (3.1.14) should also be applicable to the portables. In subsequent simulations, we assume the portables are randomly distributed over a circular region. The performance is averaged over different combinations of portable locations. Thus, the constraint in (3.1.14) is usually satisfied for the portables, and it is unlikely to get into these pathological cases.

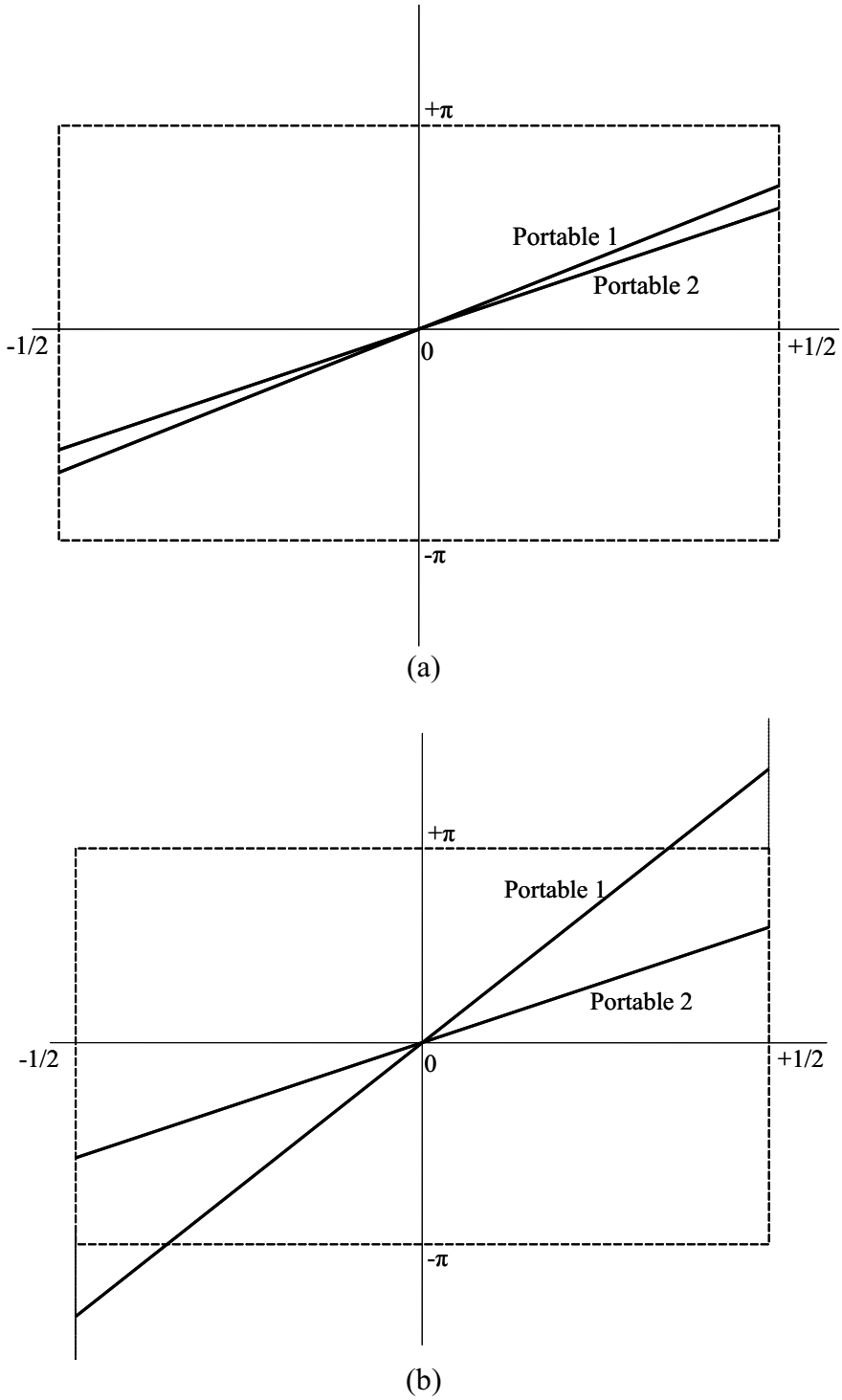

Figure 3.2.1 Linear phase difference versus the normalized frequency, (a) similar slopes, (b) disparate slopes.

3.3 Evaluation Using Condition Numbers

The condition number of the channel matrix can be quickly obtained to show either the matrix is good or bad. Its value is consistent with the intuition: when the BS antennas are far apart, the superposition of signals are different and the condition number is samll; when the antennas are close, the superposition of signals at the antenna is close and the condition number is big. Therefore, we strive for smaller condition numbers in order to achieve spatial multiplexing. There is no direct connection between the condition number and the actual performance of the equalizers. However, the channel matrix has captured all the different delay terms and they are the cause of the separable signals. It is expected that any equalizer would benefit from large antenna separation.

The condition number of a linear system is defined as

$$\kappa = \|H(f)\| \left\|H(f)^{-1}\right\|, \tag{3.3.1}$$

where $\|\bullet\|$ denotes the matrix norm. The 2-norm condition number of $H(f)$ can be found from the ratio between the largest and the smallest eigenvalue of $H(f)^H H(f)$, where $\bullet^H$ is the Hermitian operator. For the two-portables two-receive-antenna case, we have

$$H(f)^H H(f) = \begin{bmatrix} 2 & e^{j2\pi f(\tau_{11}-\tau_{12})} + e^{j2\pi f(\tau_{21}-\tau_{22})} \\ e^{j2\pi f(\tau_{12}-\tau_{22})} + e^{j2\pi f(\tau_{22}-\tau_{21})} & 2 \end{bmatrix}. \tag{3.3.2}$$

After straightforward algebraic manipulation, we obtain

$$\kappa^2 = \frac{1+\left|\cos\pi f\left(\tau_{11}-\tau_{12}+\tau_{22}-\tau_{21}\right)\right|}{1-\left|\cos\pi f\left(\tau_{11}-\tau_{12}+\tau_{22}-\tau_{21}\right)\right|}. \tag{3.3.3}$$

Therefore, we have

$$\kappa = 1 \quad \text{when} \quad \cos \pi f \left(\tau_{11} - \tau_{12} + \tau_{22} - \tau_{21} \right) = 0 , \tag{3.3.4a}$$

$$\text{and} \quad \kappa = \infty \, \text{when} \quad \cos \pi f \left(\tau_{11} - \tau_{12} + \tau_{22} - \tau_{21} \right) = \pm 1 . \tag{3.3.4b}$$

The condition number is a function of difference in delays and frequency. The first simulation scenario, as described in Fig. 3.1.1(a), investigates the relation between the condition number and two portable locations. The frequency is fixed at $1/2T_g$. The two receive antennas are symmetrically located at the centre of a circular region with a radius of 100 λ_g. The reason behind this is that the radius should be at least greater than twice the separation between receive antennas to avoid limiting the portables to a constrained region. Further increasing the radius is of no concern. It is the difference in delays that matters, but not the actual distance. Fig. 3.3.1 to Fig. 3.3.6 show the log of the condition numbers[5] against the portable locations specified by angles θ_1 and θ_2 and different BS antenna separation on the scale of signalling length.

The large values along the two diagonals of all these figures correspond to the pathological situations of (1) and (2) as described in Section 3.2, and their intersection corresponds to case (3). The value of the condition numbers away from the pathological regions decreases as the antenna separation increases to one signalling length, as in Fig. 3.3.1 to Figure 3.3.4. When the separation is equal to one signalling length in Fig. 3.3.4, there are four peaks appearing at [0, π], [π , 0], [π, 2π], and [2π, π]. This can be explained by observing the equivalence of the condition (3.3.4b) under which the condition numbers approach infinity

5. Putting the condition numbers in logarithmic scale avoids astronomical values.

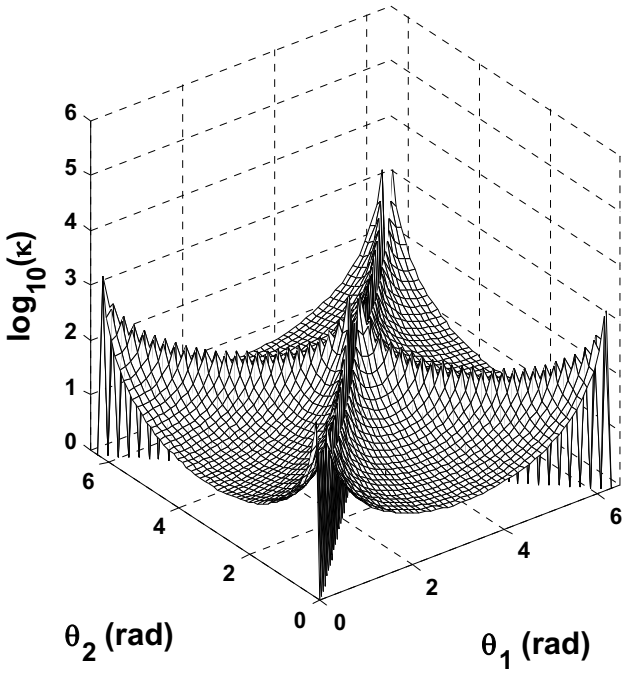

(a)

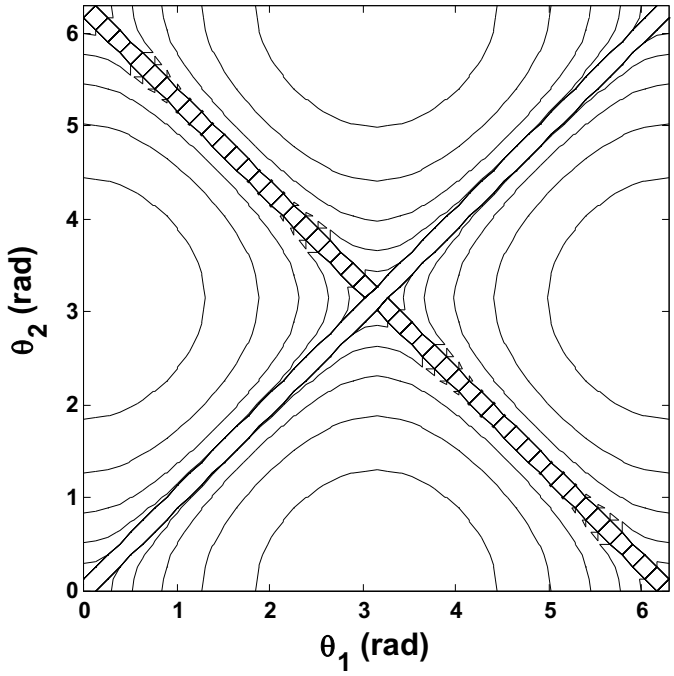

(b)

Figure 3.3.1 Log of condition numbers against different portable locations and $\Delta = 0.1\ \lambda_g$, (a) isotropic view, (b) planar view.

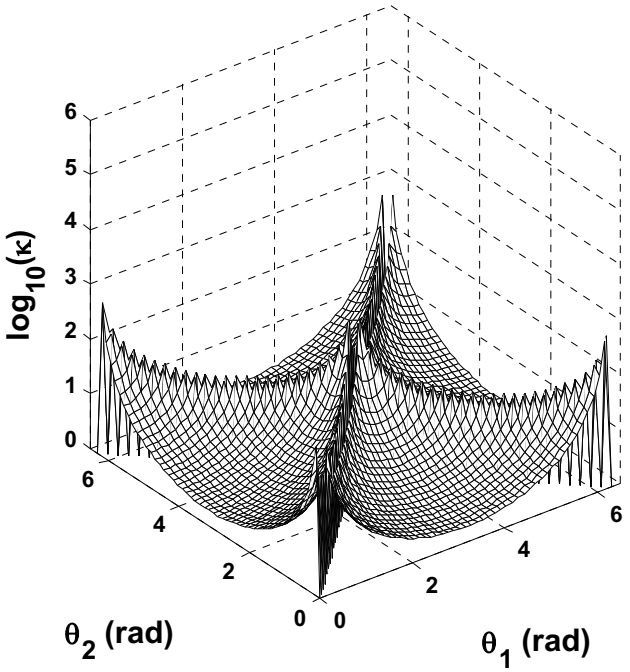

(a)

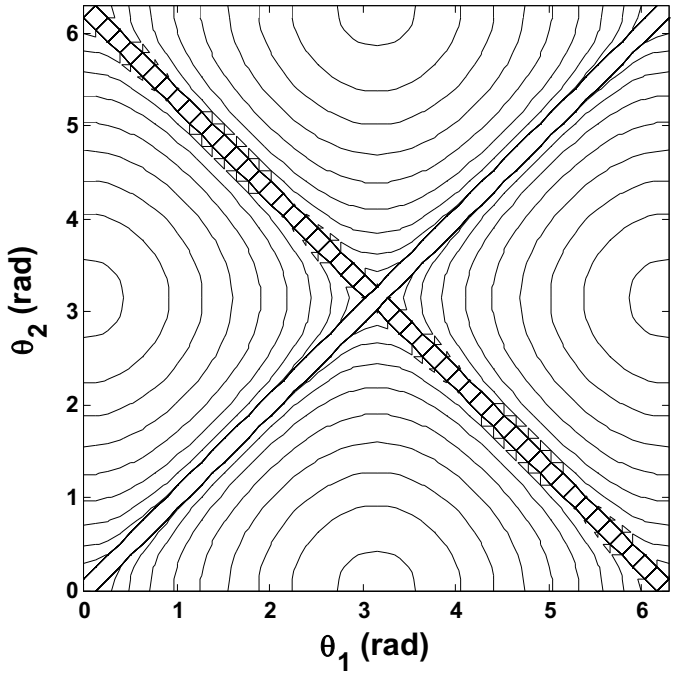

(b)

Figure 3.3.2 Log of condition numbers against different portable locations and $\Delta = 0.3\ \lambda_g$, (a) isotropic view, (b) planar view.

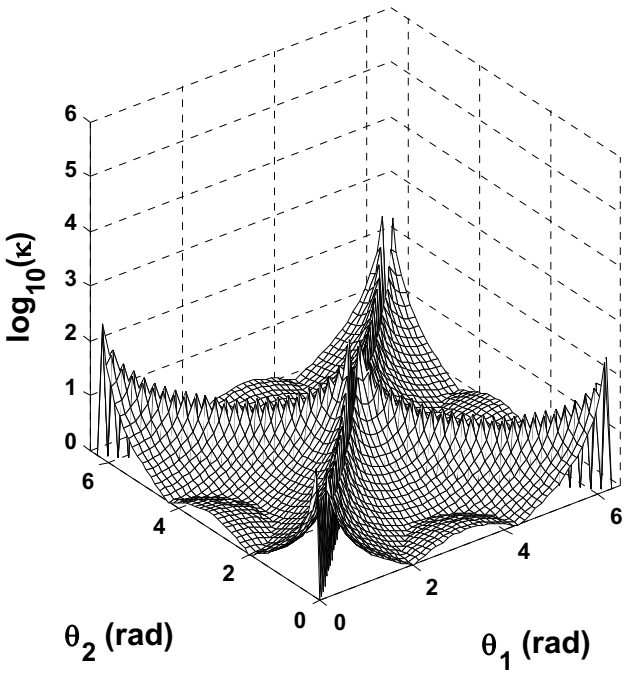

(a)

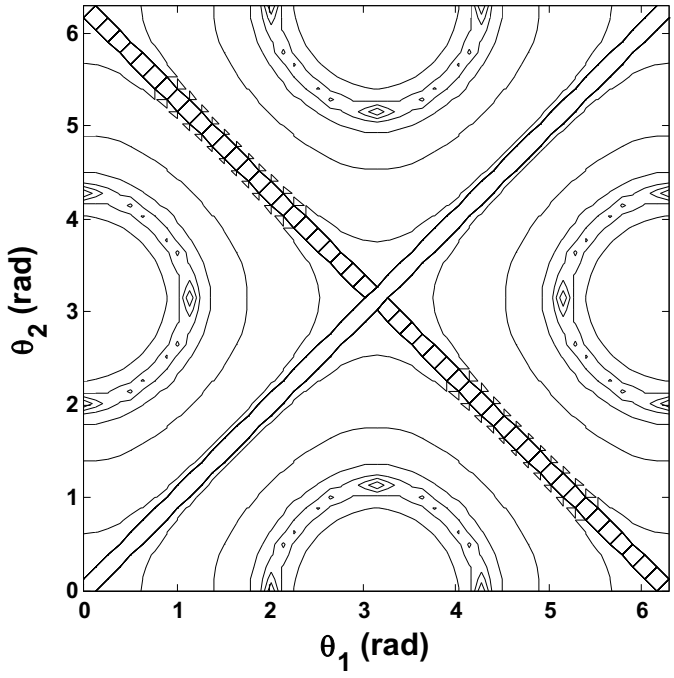

(b)

Figure 3.3.3 Log of condition numbers against different portable locations and $\Delta = 0.7\ \lambda_g$, (a) isotropic view, (b) planar view.

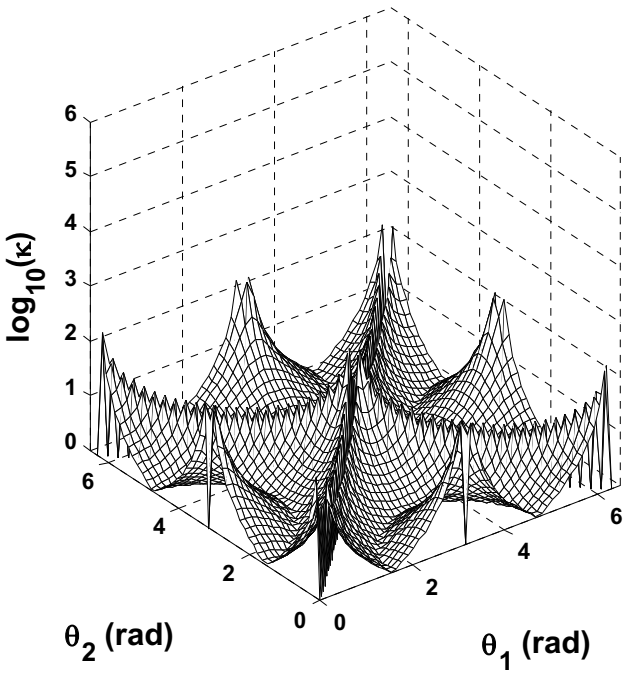

(a)

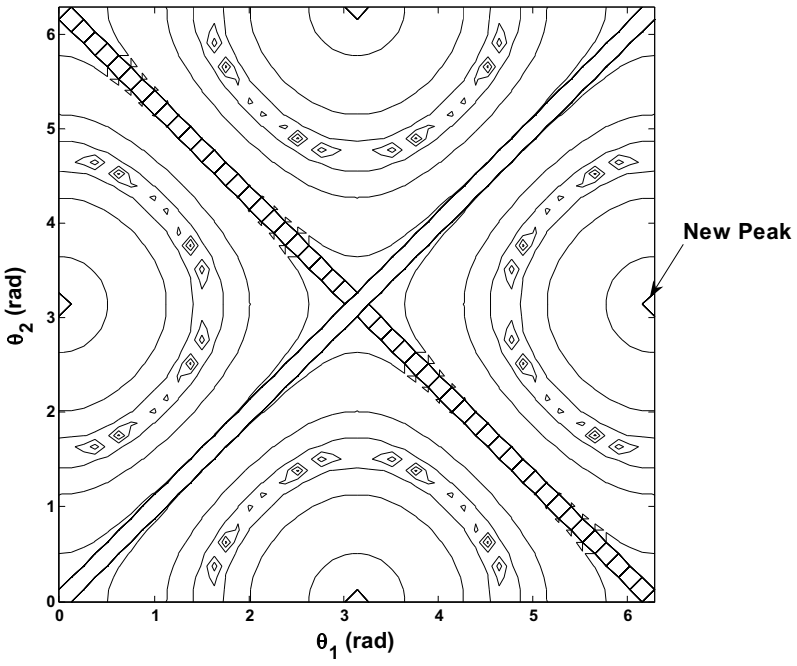

(b)

Figure 3.3.4 Log of condition numbers against different portable locations and $\Delta = 1\ \lambda_g$, (a) isotropic view, (b) planar view.

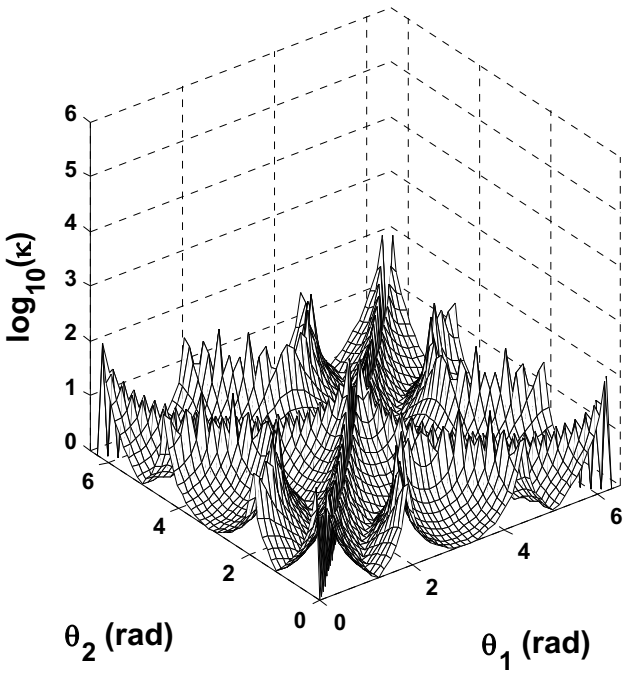

(a)

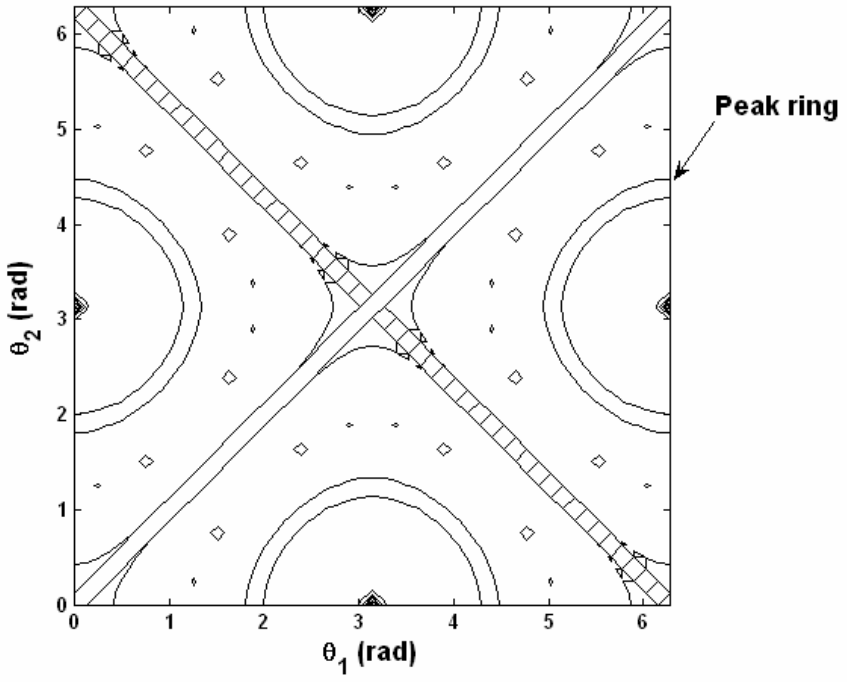

(b)

Figure 3.3.5 Log of condition numbers against different portable locations and $\Delta = 1.5\ \lambda_g$, (a) isotropic view, (b) planar view.

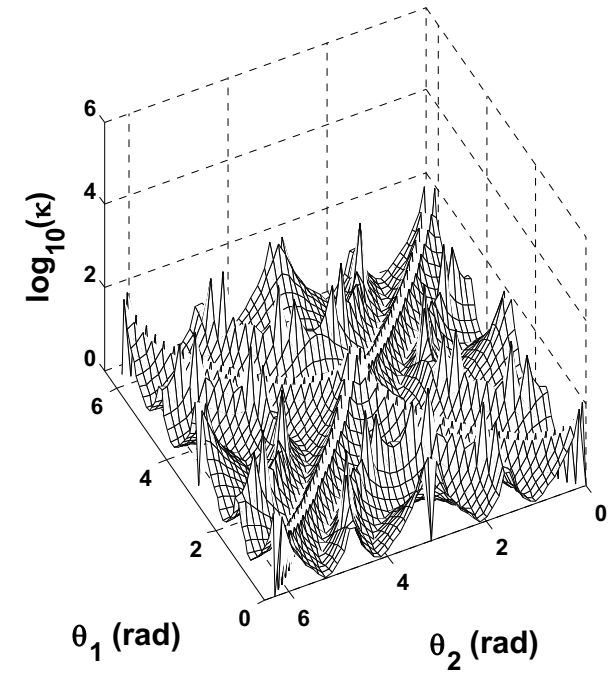

(a)

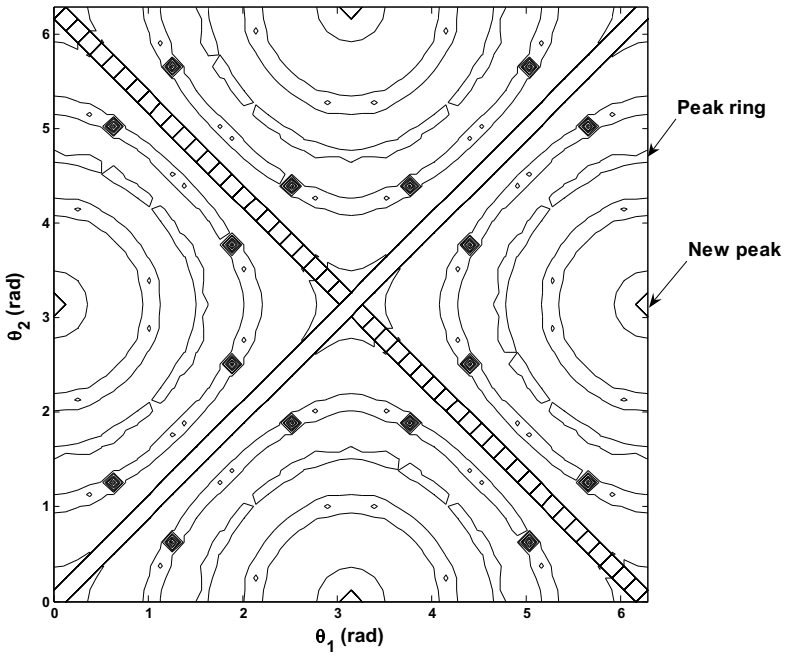

(b)

Figure 3.3.6 Log of condition numbers against different portable locations and $\Delta = 2\,\lambda_g$, (a) isotropic view, (b) planar view.

$$\pi f\left(\tau_{11} - \tau_{12} + \tau_{22} - \tau_{21}\right) \;=\; x\pi \tag{3.3.5}$$

where x is an integer. This can be further expressed as

$$\frac{\pi}{2}\left[\left(l_{11}-l_{12}\right)/\lambda_g+\left(l_{22}-l_{21}\right)/\lambda_g\right] = x\pi \text{, where } f=\frac{1}{2T_g}. \qquad (3.3.6)$$

When the portables are at those four locations, we have the relations $|l_{11}\text{-}l_{12}| = \lambda_g$ and $|l_{22}\text{-}l_{21}| = \lambda_g$. which can be shown to satisfy (3.3.6). Therefore, the condition numbers approach infinity. As the antenna separation further increases as in Fig. 3.3.5 and Fig. 3.3.6, there are more combinations of locations along the circle to satisfy (3.3.6). We observe the peaks spread out to form a half ring, and new peaks are formed at the four locations whenever the separation exceeds an integer multiple of a signalling length**.** These peaks correspond to bad condition numbers at a particular combination of portable locations and at a particular frequency. They will be of less significance if the equalizers are optimized according to other statistical criteria, such as the minimum mean squared error.

The second simulation scenario is to fix the two portable locations on the circle. Fig. 3.3.7 shows a set of plots of the log of the condition numbers against the frequency normalized with respect to $1/T_g$ at different antenna separations. Condition number is an even function with respect to frequency. We can see an increase in the antenna separation from 0.005 λ_g to λ_g significantly shifts the overall condition numbers downward, while there is marginal improvement as the separation increases to 3 λ_g. In addition, there are also peaks at certain frequencies and they appear more often as the separation goes beyond one signalling length. They

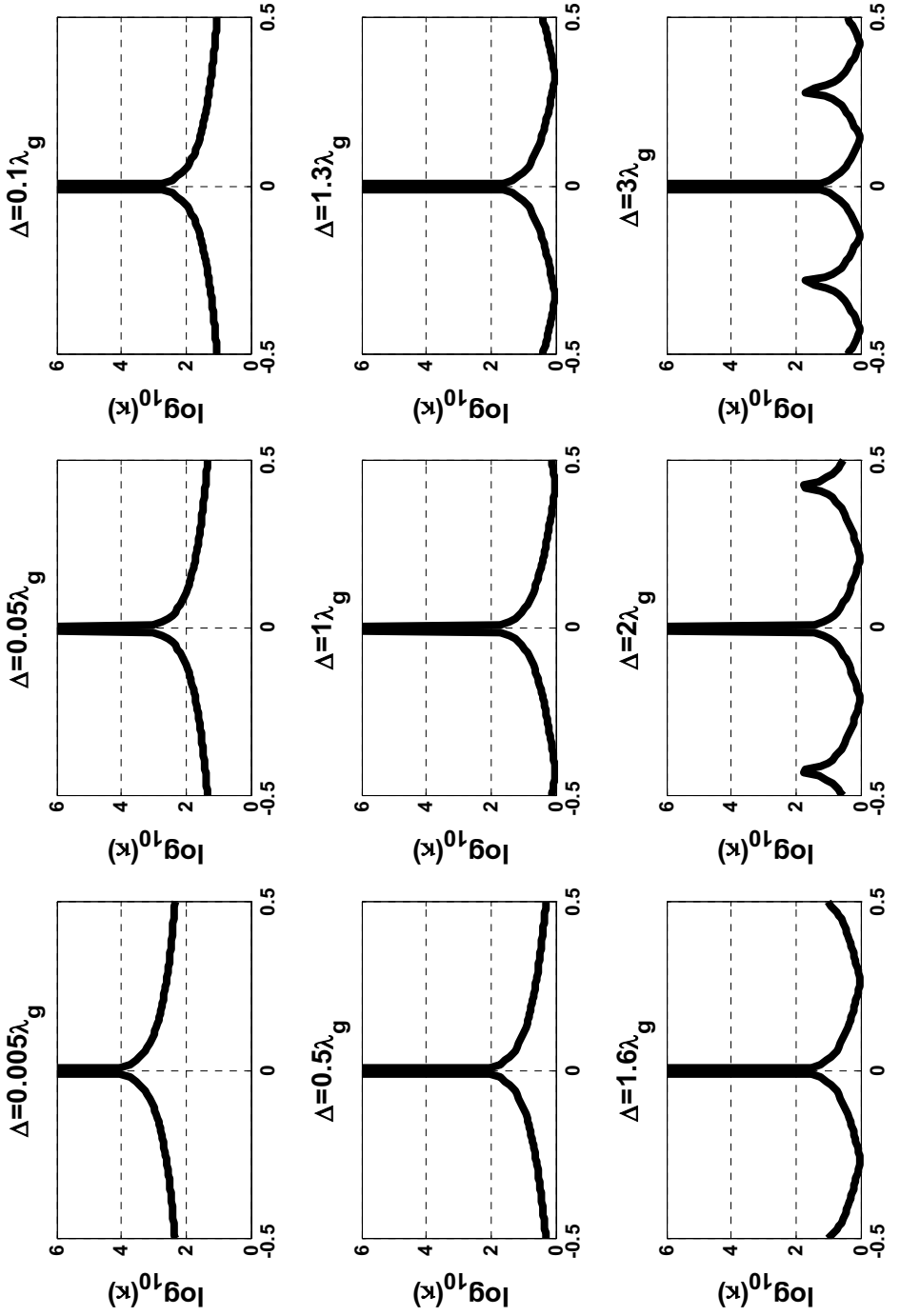

Figure 3.3.7 Log of condition numbers versus the normalized frequency at different Δ.

correspond to the occasions that (3.3.6) is satisfied. The peaks at the center correspond to the case when frequency is zero.

The condition number is a function of both portable locations and frequency. Fig. 3.3.1 to Fig. 3.3.7 have indicated the improvement in condition numbers due to antenna separation by the signalling length. However, it is difficult to directly visualize its impact, particularly with the presence of occasional peaks when the separation exceeds one signalling length. Therefore, we turn to statistical averaging to eliminate these sporadic behaviors and isolate the effect of antenna separation only. The portable locations are kept the same as in the second simulation. We take the values of the log of the condition numbers of 100 equispaced points over $[-1/2T_g, +1/2T_g]$ to generate one histogram in Fig. 3.3.8 and compute the mean. Fig. 3.3.8 shows a set of the histograms and the mean values at different antenna separations. The density of the histogram shifts towards smaller condition numbers as antenna separation increases. Therefore, the mean of the log of the condition numbers at each antenna separation is a good figure of merit to show the channel improvement.

In the third simulation, the portables are uniformly distributed on a circle of radius 200 λ_g. A thousand sets of locations are collected. The mean of the log of the condition numbers is calculated over the normalized frequency for each set of portable locations. Then the average of the 1000 means is calculated and plotted for a particular antenna separation. Fig. 3.3.9 shows the effect of antenna separation on the average of the mean of the log of condition numbers. We observe a steep decline in the condition number from fractions of one signalling length to one signalling

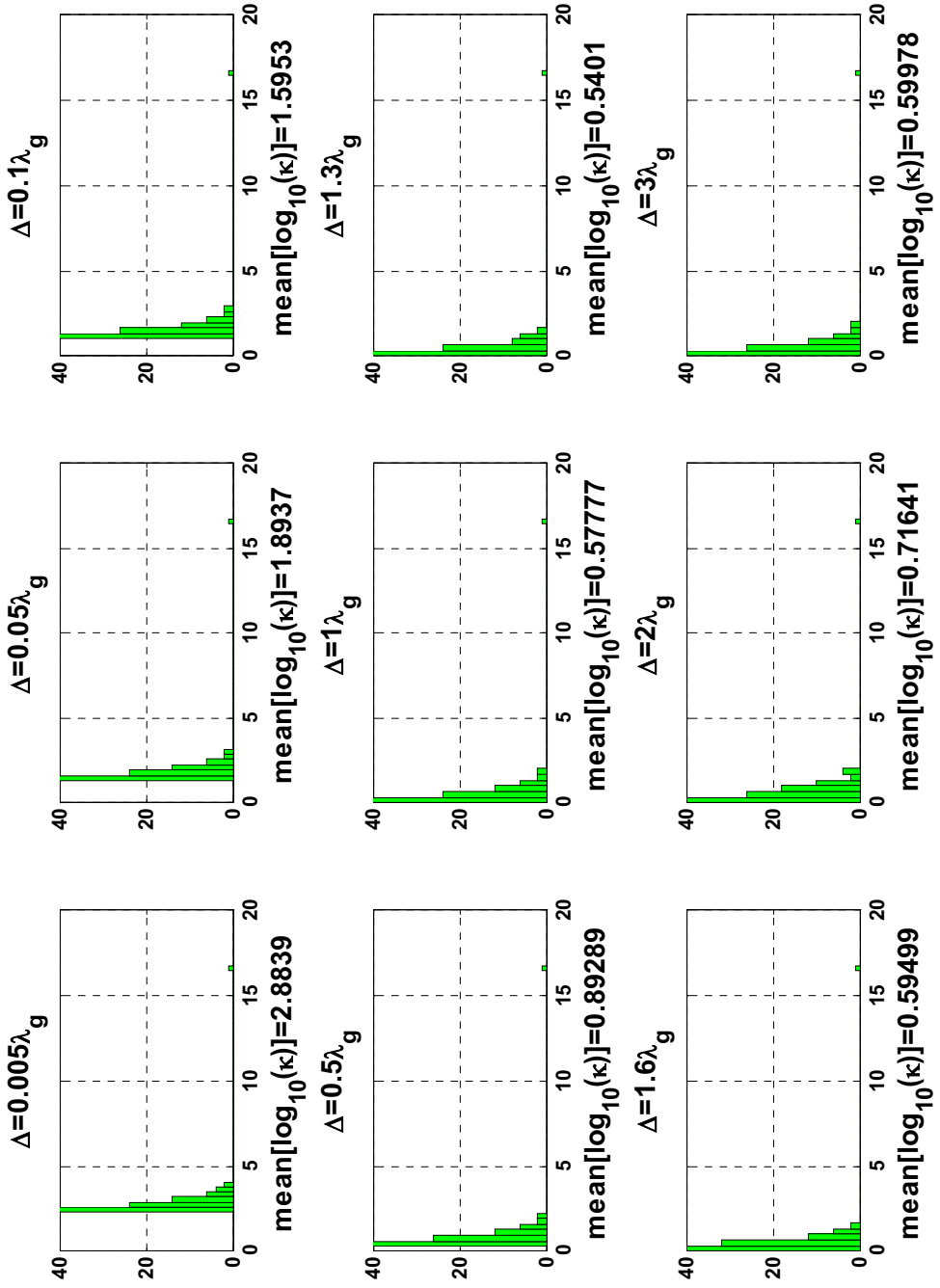

Figure 3.3.8 Histogram of the log of condition numbers at different Δ.

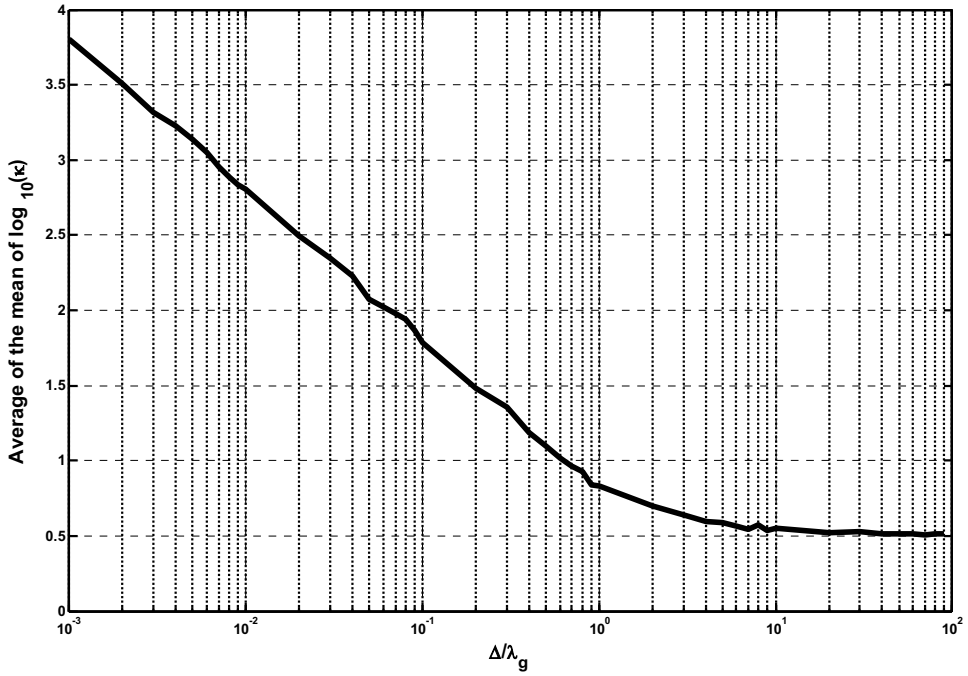

Figure 3.3.9 Mean of the log of condition numbers averaged over 1000 sets of portable locations versus Δ.

length. This confirms our intuition that, the separation on the scale of carrier wavelength incurs difficulty to identify signals in LOS pure-delay channels. It is more appropriate to separate antennas on the scale of signalling length in order to get a channel matrix with lower sensitivity to errors. In addition, Fig. 3.3.9 shows a diminishing return as the antenna separation increases further beyond a few signalling length. In those cases, the two linear phase differences will be wrapped around several times for most portable locations due the cyclic behavior over [$-\pi$, $+\pi$], and appear uncorrelated at each frequency. Simulation of the three-portable-three-receive antenna scenario also confirms this trend.

3.4 Analysis of Interference Correlation

This section presents the analysis of correlated interference similar to the work of Yanikomeroglu et al. but for non-spread systems. Their analysis concentrates on the signals while our analysis concentrates on the channel matrix. The receiver structure is shown in Fig. 3.4.1 in which a chip level correlator is replaced by a symbol-oriented ideal non-causal matched filter. The difference between this receiver and the one in Fig. 2.2.1 is that the receive filters are pure delays $\delta(t+\tau_{11})$ and $\delta(t+\tau_{12})$, to synchronize the desired signal to the same time instance in order to maximize the signal power. Together with the weights, this receiver performs MRC rather than equalization as considered in our case. We may interpret the combination of the delays and the weights as "filters". But they are simpler in contrast with the filters obtained by inverting (3.1.1)

$$R_{11}(f) = \frac{e^{-j2\pi f\tau_{22}}}{e^{-j2\pi f(\tau_{22}+\tau_{11})} - e^{-j2\pi f(\tau_{21}+\tau_{12})}}, \qquad (3.4.1a)$$

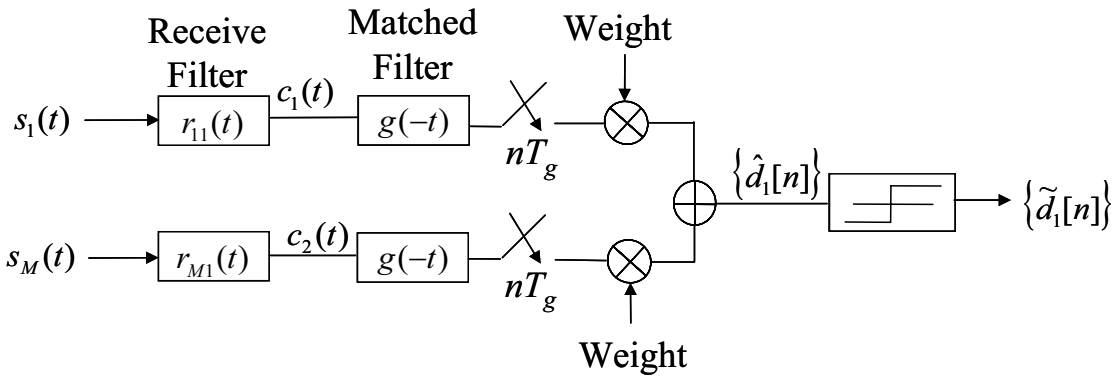

Figure 3.4.1 Receiver for correlated interference analysis.

and

$$R_{21}(f) = \frac{-e^{-j2\pi f\tau_{21}}}{e^{-j2\pi f(\tau_{22}+\tau_{11})} - e^{-j2\pi f(\tau_{21}+\tau_{12})}}. \qquad (3.4.1b)$$

The performance of this receiver is expected to be worse than the one considered in our case.

Let us assume the portables are transmitting at the same time. The received signals at the two branches are

$$s_1(t) = u_1(t-\tau_{11}) + u_2(t-\tau_{21}), \qquad (3.4.2a)$$

$$s_2(t) = u_1(t-\tau_{12}) + u_2(t-\tau_{22}). \qquad (3.4.2b)$$

The outputs after the pure delay filters become

$$c_1(t) = u_1(t) + u_2(t-T_I), \text{ where } T_I = \tau_{11} - \tau_{21}, \qquad (3.4.3a)$$

$$c_2(t) = u_1(t) + u_2(t-T_{II}), \text{ where } T_{II} = \tau_{12} - \tau_{22}. \qquad (3.4.3b)$$

The first terms in (3.4.3) are the signal and the second terms in (3.4.3) are the interference. Assume the transmitted signals are square waveforms, then the matched filter becomes

$$g(t) = 1, \text{ where } t \in [0, T], \qquad (3.4.4a)$$

$$g(t) = 0, \text{ otherwise.} \qquad (3.4.4b)$$

After the matched filter, the interference Z_1 of the first branch becomes

$$Z_1 = \int_0^{T_I} g(t) d_2[n-1]\, dt + \int_{T_I}^{T_g} g(t) d_2[n]\, dt,$$

$$= T_I d_2[n-1] + (T_g - T_I) d_2[n], \text{ where } T_I \in [0, T_g]. \qquad (3.4.5a)$$

For other time intervals of T_I, we have

$$Z_1 = (T_I - T) d_2[n-2] + (2T_g - T_I) d_2[n-1], \text{ where } T_I \in [T_g, 2T_g], \qquad (3.4.5b)$$

$$Z_1 = (T_I + T)\, d_2[n] + (-T_I)\, d_2[n+1], \text{ where } T_I \in [-T_g, 0], \quad (3.4.5c)$$

$$Z_1 = (T_I + 2T)\, d_2[n+1] + (-T_g - T_I)\, d_2[n+2], \text{ where } T_I \in [-2T_g, -T_g]. \quad (3.4.5d)$$

The interference Z_2 of the second branch after the matched filter has the same expression as in (3.4.5). The interference Z_1 and Z_2 are regarded as random variables, and they have zero mean. Since the binary data are uncorrelated due to time shift (2.1.4), the variance of Z_1 is

$$E[Z_1^2] = (T_I - T_g)^2 + (2T_g - T_I)^2, \text{ where } T_I \in [T_g, 2T_g], \quad (3.4.6a)$$

$$E[Z_1^2] = (T_I)^2 + (T_g - T_I)^2, \text{ where } T_I \in [0, T_g], \quad (3.4.6b)$$

$$E[Z_1^2] = (T_I)^2 + (T_g + T_I)^2, \text{ where } T_I \in [-T_g, 0], \quad (3.4.6c)$$

$$E[Z_1^2] = (T + T_I)^2 + (2T_g + T_I)^2, \text{ where } T_I \in [-2T_g, -T_g]. \quad (3.4.6d)$$

And the variance of Z_2 of the second branch has the same expression as in (3.4.6) over different intervals of T_{II}. We are interested in the correlation of Z_1 and Z_2. If they are completely correlated, combining after the unity weights enhances both the signal and the interference. Their correlation $E[Z_1 Z_2]$ over different combinations of the time intervals of T_I and T_{II} is listed in Table 3.4.1, and the correlation coefficient ρ is shown in Fig. 3.4.2. We can see from Fig. 3.4.2, for $T_I \in [nT_g, (n+1)T_g]$,

$$\rho = 0, \text{ where } T_{II} \in [(n-1)T_g, (n+2)T_g], \quad (3.4.7a)$$

$$\rho \neq 0, \text{ otherwise.} \quad (3.4.7b)$$

T_I and T_{II} are dependent on the specific location of the portables. Given the location of the first portable, we can find the region of the second portable in which the

$E[Z_1 Z_2]$	$T_I \in [-2T_g, -T_g]$	$T_I \in [-T_g, 0]$	$T_I \in [0, T_g]$	$T_I \in [T_g, 2T_g]$
$T_{II} \in [-2T_g, -T_g]$	$(2T_g + T_I)(2T_g + T_{II}) + (T_g + T_I)(T_g + T_{II})$	$(-T_I)(2T_g + T_{II})$	0	0
$T_{II} \in [-T_g, 0]$	$(-T_{II})(2T_g + T_I)$	$(T_g + T_I)(T_g + T_{II}) + (T_I)(T_{II})$	$(T_g + T_{II})(T_g - T_I)$	0
$T_{II} \in [0, T_g]$	0	$(T_g + T_I)(T_g - T_{II})$	$(T_g - T_I)(T_g - T_{II}) + (T_I)(T_{II})$	$(2T_g + T_I)(T_{II})$
$T_{II} \in [T_g, 2T_g]$	0	0	$(2T_g - T_{II})(T_I)$	$(2T_g - T_I)(2T_g - T_{II}) + (T_g - T_I)(T_g - T_{II})$

Table 3.4.1 Interference correlation over different time intervals of T_I and T_{II}.

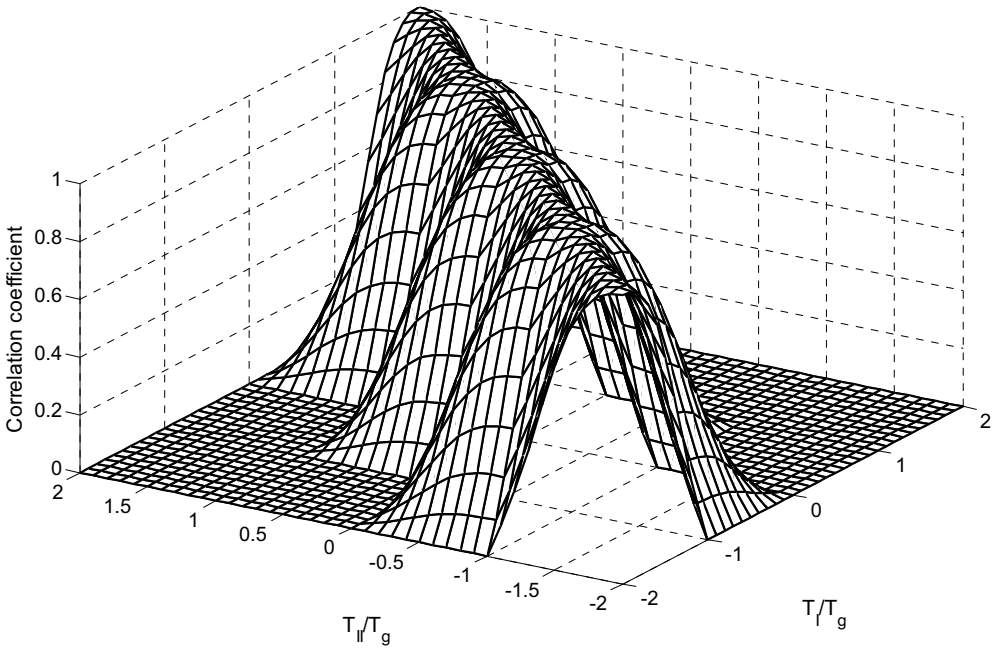

Figure 3.4.2 Correlation coefficient as a function of T_I and T_{II}.

interference correlation is high.

The region is named the caution zone by Yanikomeroglu et al.. The authors have showed the caution zone is bounded by two hyperbolas in the two portable two receive antenna scenario, and it gets narrower as the separation between antennas increase. Therefore, they conclude "to minimize the caution zone (and the effects of the correlated interference), antenna elements must be placed as far apart as possible." However, our simulation has pointed out that there is diminishing return once the separation is beyond a few signalling length.

3.5 Applications of Signalling Length

The constraints on signalling length are applicable to digital wireless communication systems which use multiple antennas to combat CCI. In those systems which operate in environment with long coherent distances[6], the signal envelopes at the receive antennas would be highly correlated, and the effect due to antenna separation should be prominent.

3.5.1 Local Multipoint Communication Systems

The Local Multipoint Communication System (LMCS) is a fixed broadband TDMA wireless system providing services such as wireless cable TV, video telephony, video conferencing, and video-on-demand to homes [Sta96]. Its operating frequency is around 28 GHz with a typical reverse link bit rate of 2 to 10 Mbps. These correspond to 0.0107 m in carrier wavelength and 30 to 150 m in signalling length. The field measurements for LMCS by Roy et al. report very high correlation with antenna separation around 100 λ_c, and even as large as 1000 λ_c (corresponds to

6. Coherence distance is defined as the distance over which the correlation coefficient of signal envelopes at two separated antennas is above a certain value, e.g. 0.5.

approximately 10 m and 1/3 λ_g) in which cases, the angle of the transmit antenna is about 0º relative to the linearly located receive antennas [Roy00, ch. 3]. The author considered one desired transmitted signal with another interfering signal, and used his channel model devised for LMCS in the simulation. He used four linearly spaced receive antennas followed by a linear equalizer. The bit-error-rate (BER) plot [Roy00, ch. 5] averaged over random transmitter locations shows improvement with separation from 1 λ_c to 100 λ_c (corresponds to approximately 1 m and 1/30 λ_g). The factor, 1/30, with respect to the signalling length is minute, but the separation has contributed to this improvement.

3.5.2 Very Wide Band Systems

In addition to searching for an appropriate environment, we can also identify applications having very high signalling rates and very short signalling length. The reasoning is as follows. Assume an environment full of reflecting objects. For narrowband signals that have the relation $f_c >> f_g$, each element in the two by two channel matrix is a complex Gaussian random variable. Even without the difference in delays, the randomness of these elements allows an easy separation of signals from interference. Therefore, separation on signalling length is not meaningful. For wideband signals with a lower frequency, f_1, and an upper frequency, f_2, and the relation $f_2 > f_1 > f_g$, the story is similar. Each element of the channel matrix becomes a function of frequency. Due to the assumption of rich reflections, we can apply the idea of uncorrelated fading on the carrier frequency to the lower and upper frequencies. At each of these frequencies, the matrix elements are random. The separation on the lower wavelength λ_1 is sufficient to ensure the matrix elements are random for all

other frequencies above. Since we have the relation $\lambda_2 < \lambda_1 < \lambda_g$, separation on signalling length is still not necessary.

The scenario changes when signals are very wide band and the frequency relation becomes $f_2 > f_g > f_1$. We may still separate on λ_1 for uncorrelated fading for all frequencies. However, we would already have the effect of different delays due to the relation $\lambda_1 > \lambda_g$. Separation on the signalling length incurs uncorrelated fading for the range $[f_g, f_2]$, and incurs disparate phase for the range $[f_1, f_g]$. Together, we can separate the signal from interference without heeding λ_1. The power spectrum density of the signals in these three different scenarios are illustrated in Fig. 3.5.1. The Ultra Wideband (UWB) systems may satisfy the relation $f_2 > f_g > f_1$. In 2002, the Federal Communications Commission (FCC) allocated a wide spectrum from 3.1 to 10.6 GHz for it [FCC02]. This corresponds to a signalling length being a fraction of a meter. UWB systems generally use spreading codes to differentiate users since the chip rate can be very high. However, if multiple antennas are used to combat interference, the separation will be on the scale of signalling length or chiplength. In addition, it is mentioned in [Hud81, ch.2] that sonar arrays are wideband and their aperture is comparable to the signalling length. Our results may also be applicable here.

(a)

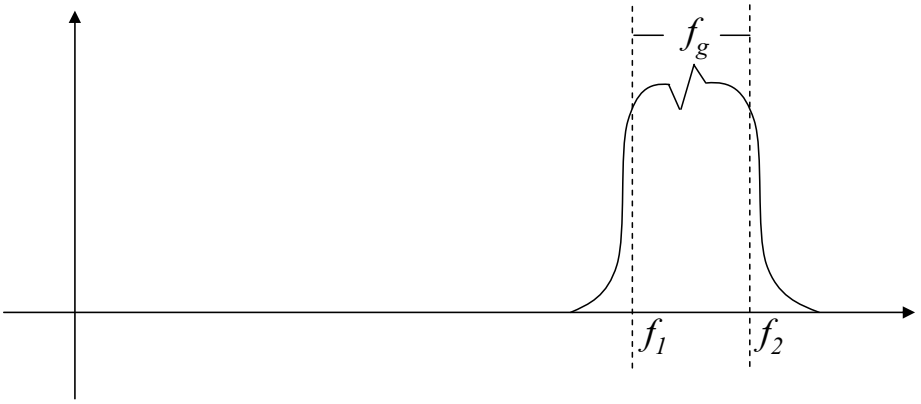

(b)

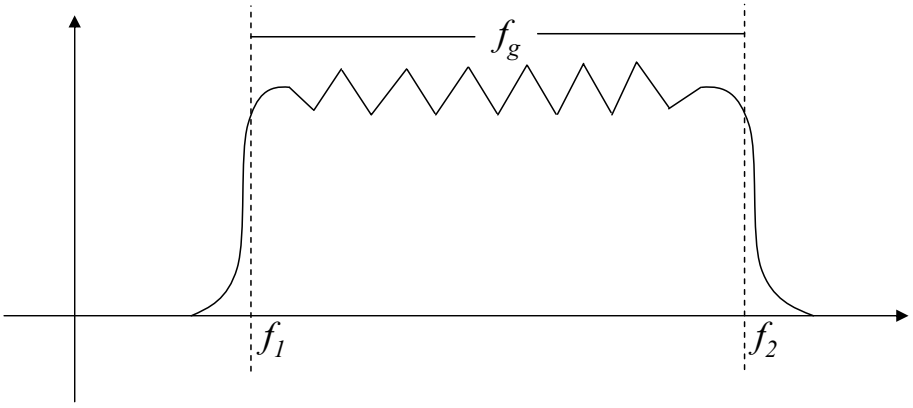

(c)

Figure 3.5.1 Power spectrum density of signals with different bandwidth, (a) narrowband, $f_c >> f_g$ and $\lambda_c << \lambda_g$, (b) wideband, $f_2 > f_1 > f_g$ and $\lambda_2 < \lambda_1 < \lambda_g$, (c) very wide band, $f_2 > f_g > f_1$ and $\lambda_2 < \lambda_g < \lambda_1$.

Chapter 4 Summary and Future Work

4.1 Summary

This thesis presents the reasoning of a newly defined parameter signalling length, which is used as a measure of the separation between antennas. The analysis is from the perspective of exploiting spatial multiplexing from multiple antennas in LOS pure-delay environment. This requires our non-spread system model to include equalizers.

We showed the existence of linear equalizers optimized to the ZF criterion and they are the inverse of the channel matrix. Then, we looked at how the delays affect the row dependencies of the channel matrix and reasoned that the speration between BS antennas should be at least greater than a signalling length in order to achieve diverse phase relationships. Next, we used condition numbers to indicate the good and the bad channel matrix. However, the analysis in the frequency domain showed occasional astronomical values in the condition numbers. To cope with that, we used the mean of the condition numbers to reflect the effect of different antenna separations. Simulations have confirmed our reasoning to separate on the scale of signalling length. Even though we have assumed ideal channel conditions, two digital wireless radio systems are discussed in which the antenna separation should be measured on the scale of signalling length. The key characteristics are long coherent distance in channels, and very wide bandwidth in the signals. The second characteristic naturally leads to spread spectrum systems.

4.2 Future Work

Neither the correlation of interference in [Yan02] nor the mean of condition numbers in our analysis is the true measure of the equalizer performance. However, they directly reflect the effect of antenna separations on the scale of a signaling length, and they lead to analytical expressions as shown in Table 3.4.1 and (3.3.3). It is expected that they vary proportionally with respect to the true performance. However, this can only be confirmed through simulations to get the BER plots. Also, Yanikomeroglu et al. claims that the antenna elements must be placed as far apart as possible, while we observed diminishing return once the separation is beyond a few signalling length. This disparity can also be answered from these BER plots.

The presented results are drawn from the two-portable two-receive-antenna scenario. Only one dimension, the distance between two antennas is investigated. The next step is to look at systems with multiple antennas, and identify their proper geometric layout from the perspective of achieving spatial multiplexing through different phase. This will be different from other optimizing criteria on antenna arrays such as maximizing diversity gain [Lia95], isotropic direction of arrival estimation [Bay03]. Future work in this direction, as pointed out by Yanikomeroglu et al., may lead to the creation of a "spatial sampling theorem" which can answer the question "how often should a wireless signal be collected?"

Nothing would be more exciting than being able to build a physical system to show effect of the signalling length. Since the UWB technology promises large bandwidth and short signalling length, the implication of signalling length in UWB multi-antenna systems can be a research direction. However, care must be exercised

over its current specification, such as modulation techniques and emission power [Por03] [Qiu05].

References

[Bay03] Ü. Baysal and R. L. Moses, "On the Geometry of Isotropic Arrays," *IEEE Trans*. *Signal Process*., vol. 51, no. 6, pp. 1469-1478, June 2003.

[Cla68] R. H. Clarke, "A statistical theory of mobile-radio reception," *Bell Syst*. *Tech*. *J*., vol. 47, pp. 957-1000, July-Aug. 1968.

[Cla94] M. V. Clark, M. Shafi, W. K. Kennedy and L. J. Greenstein, "Optimum linear diversity receivers for mobile communications," *IEEE Trans*. *Veh*. *Technol*., vol. 43, no. 1, pp. 47-56, Jan. 1994.

[Ert98] R. B. Ertel, P. Cardieri, K.W. Sowerby, T. S. Rappaport and J. H. Reed, "Overview of spatial channel models for antenna array communication systems," *IEEE Pers*. *Commun*., vol. 5, no. 1, pp. 10-22, Feb. 1998.

[Fal00] D. Falconer, A. Legnain and S. Roy, "Receiver spatial-temporal signal processing for broadband wireless systems," in *Proc*. *PRIMC*, 2000, pp. 676-682.

[FCC02] Revision of Part 15 of the Commission's Rules Regarding Ultra-Wideband Transmission Systems First Report and Order. Washington, D. C. [Online]. Retrieved June 27, 2005, from http://hraunfoss.fcc.gov/edocs_public/attachmatch/FCC-02-48A1.pdf

[Hud81] J. E. Hudson, *Adaptive Array Principles*. Stevenage, UK: Peter Peregrinus Ltd., 1981.

[Jak94] W. C. Jakes, *Microwave Mobile Communications*, *Second Edition*, Piscataway, NJ, USA: IEEE Press, 1994.

[Lia95] J. Liang and A. J. Paulraj, "On optimizing base station antenna array topology for coverage extension in cellular radio networks," in *Proc. VTC*, 1995, pp. 866-870.

[Qiu05] R. C. Qiu, H. Liu and X. Shen, "Ultra-wideband for multiple access communications," *IEEE Commun. Mag.*, vol 43, no. 2, pp. 80-87, Feb. 2005.

[Pau03] A. J. Paulraj, R. Nabar and D. Gore, *Introduction to Space-Time Wireless Communications*, Cambridge, UK: Cambridge University Press, 2003.

[Por03] D. Porcino and W. Hirt, "Ultra-wideband radio technology: potential and challenges ahead," *IEEE Commun. Mag.* vol. 41, no. 7, pp. 66-74, July 2003.

[Pro95] J. G. Proakis, *Digital Communications*, *Third Edition*, New York, NY, USA: McGraw-Hill, Inc., 1995.

[Roy00] S. Roy, *Space-Time Processing in Fixed Broadband Wireless Systems*. PhD thesis, Dept. of Systems and Computer Engineering, Carleton University, Ottawa, ON, Canada, Aug. 2000.

[Sal93] J. Salz and J. H. Winters, "Effect of fading correlation on adaptive arrays in digital wireless communications," in *Proc. ICC*, 1993, pp. 1768-1774.

[Skl01] B. Sklar, *Digital Communications Fundamentals and Applications*, *Second Edition*, Upper Saddle River, NJ, USA: Prentice-Hall, Inc., 2001.

[Sta96] G. M. Stamatelos and D. D. Falconer, "Millimeter radio access to multimedia services via LMDS," in *Proc. Globecom*, 1996, pp.

1603-1607.

[Shn67] D. A. Shnidman, “A generalized Nyquist criterion and an optimum linear receiver for a pulse modulation system,” *Bell Syst. Tech. J.*, vol. 46, no. 9, pp. 2163-2177, Nov. 1967.

[Vau93] R. G. Vaughan and N. L. Scott, “Closely spaced monopoles for mobile communications,” *Radio Sci.*, vol. 28, no. 6, pp. 1259-1266, Nov.-Dec. 1993.

[Win84] J. H. Winters, “Optimum combining in digital mobile radio with cochannel interference,” *IEEE J. Select. Areas Commun.*, vol. SAC-2, no. 4, pp. 528-539, July 1984.

[Win87] J. H. Winters, “Optimum combining for indoor radio systems with multiple users,” *IEEE Trans. Commun.*, vol. 35, no. 11, pp. 1222-1230, Nov. 1987.

[Yan02] H. Yanikomeroglu and E. S. Sousa, “Antenna gain against interference in CDMA macrodiversity systems,” *IEEE Trans. Commun.*, vol. 50, no. 8, pp. 1356-1371, Aug. 2002.

[Zhe03] L. Zheng and D. N. C. Tse, “Diversity and multiplexing: a fundamental trade-off in multiple antenna channels,” *IEEE Trans. Info. Theory*, vol. 49, no. 5, pp. 1073-1096, May 2003.